Geologia Croatica
Journal of the Croatian Geological Survey and the Croatian Geological Society
2018 | 71/2 | 65–82 | 6 Figs. | 2 Tabs. | www.geologia-croatica.hr

Evaluations of the downward velocity of soil water movement in the unsaturated zone in a groundwater recharge area using $\delta^{18}O$ tracer: the Kumamoto region, southern Japan

Azusa Okumura[1]*, Takahiro Hosono[1], Dennis Boateng[2] and Jun Shimada[1]

[1] Kumamoto University, Priority Organization for Innovation and Excellence, 2-39-1 Kurokami, Kumamoto 860-8555, Japan; (*corresponding author: osnx.2157@gmail.com)
[2] Kumamoto University, Graduate School of Science and Technology, 2-39-1 Kurokami, Kumamoto 860-8555, Japan

doi: 10.4154/gc.2018.09

Article history:
Manuscript received December 28, 2017
Revised manuscript accepted May 28, 2018
Available online June 21, 2018

Keywords: soil water, oxygen isotope, unsaturated zone, recharge rate, infiltration time

Abstract

Water and substances from the surface infiltrate the unsaturated zone before reaching groundwater. Yet, little study has been done on the unsaturated zone due to the difficulty of sampling. A lot of studies have been carried out on the top soil down to a depth of one metre and on shallow aquifers because they are easily accessible for sampling. The unsaturated zone of the Kumamoto region recharge areas is important due to concerns about groundwater pollution from agriculture. The aim of this study was to estimate the downward velocity of soil water movement through the unsaturated zone and the recharge rate using δ18O as a tracer. Five sampling sites were selected and a core was taken from each site. The cores were cut into 0.1 m pieces and soil water was extracted from each to analyze for δD and the δ18O content. Average δD and δ18O compositions of soil water were similar to the isotopic compositions of summer precipitation. Annual average recharge rate and the downward velocity of soil water in each site were estimated by fitting a vertical δ18O profile pattern to a precipitation δ18O time series as a theoretical water displacement flow model for recharge. An estimated annual average recharge rate in the recharge area ranged from 745 to 1058 mm/yr with the annual average downward velocity of 1.37 to 2.34 m/yr. Based on the estimated downward velocity, the infiltration time for soil water to reach the aquifer was determined as ranging from 9 to 24 years, which corresponds with previous groundwater age estimations presented in an earlier published study on the same area. It was assumed that contaminants will reach aquifers in 9 to 25 years if the effects of diffusion and microbiological reaction are not taken into account.

1. INTRODUCTION

The excessive application of chemical fertilizers and manures to agricultural lands has increased the influx of substances into the ground, which eventually reach and contaminate groundwater (SPALDING et al., 1982; UMEZAWA et al., 2008; ZHANG et al., 2014). In order to identify the type of contamination, determine its extent, trace the source and extract valuable information about the groundwater such as its age, the water is sampled to measure stable isotope ratios, major and minor ion concentrations as well as trace metals. Water and substances reaching aquifers serve as a guide to determining these groundwater characteristics (DEMLIE et al., 2007; CLOUTIER et al., 2008; HOSONO et al., 2014). Usually in groundwater studies, a direct link is created between the characteristics of the groundwater and ions, isotopes and metals on the surface without taking the unsaturated zone into consideration even though substances pass through this zone before reaching groundwater. Although the unsaturated zone has not been as actively studied as groundwater, studies have been carried out over the years that give some insight into the flow processes and solute behaviour through it (BEVEN et al., 1982; GUYMON, 1994; LIN et al., 2006). General unsaturated flow processes have also been studied. Field experiments using Cl^- as a tracer were conducted on a mine waste pile (5 m high) to evaluate the infiltration rate and detect the dominant flow system in the pile (NICHOL et al., 2005). NIMMO et al. (2007) modelled unsaturated zone flow using soil science and hydrologic data. The study focused on preferential flow and the general transport time was also clarified. DELIN et al. (2017) applied rhodamine and Br tracers to a crude oil contaminated site to detect the influence of oil on the water infiltration rate in the unsaturated zone. These studies show that the plurality of flow processes such as preferential flow and matrix flow complicates water infiltration and contaminant behaviour through unsaturated media. Understanding the behaviour of water in the unsaturated zone is important for making decisions about groundwater usage and formulating mitigation measures against groundwater contamination.

One of the earliest soil water studies using water stable isotopes was performed by ZIMMERMANN et al. (1966). In this study, D_2O was sprayed on the study area as a tracer. Soil down to 1.2 m depth was sampled 4, 26, 82, 152 and 214 days after spraying for analysis. A time series hydrogen stable isotope profile of the soil water revealed that piston flow, which is the dominant flow mechanism in near saturated formation, was excellent. Several studies have also been carried out with oxygen and hydrogen stable isotopes as tracers in dry and semi-arid areas (BARNERS and ALLISON, 1983; De VRIES et al., 2000). In agriculture, soil at 1 m depth has been actively studied. However, studies on soil at far greater depths have rarely been undertaken (BHARATI et al., 2002).

Many different isotope tracers are used around the world based on the purpose and intent of a study. One of these tracers is tritium, a radioactive isotope of hydrogen. Tritium used to be a good tracer for tracking water movement through the unsatu-

Geologia Croatica

rated zone and determining groundwater age because of it abundance in the atmosphere. In the arid climate of Arizona, it was used to determine the mixing degree between shallow and deep groundwater (HARRIS, 2000). In the humid climate of Japan, it was used as a tracer to determine the recharge rate and infiltration time (KAYANE et al., 1980; SHIMADA, 1988). However, a few studies pointed out that tritium cannot be solely relied on because its concentration keeps on dropping year after year in the atmosphere (TSUJIMURA and TANAKA, 1998). Consequently, in later studies, oxygen and hydrogen isotopes were used together instead as tracers to determine recharge rates especially in Japan (YABUSAKI et al., 2011; KUDO et al., 2016). Both recharge rate and unsaturated zone infiltration velocity are important variables that provide insight into contaminant movement through the unsaturated zone.

In this study, the study area as shown in Figure 1, the Kumamoto region, is almost 100% dependent on groundwater for drinking purposes. However, the nitrate concentration has begun to build up in the water, raising concerns about groundwater contamination (HOSONO et al., 2013). The high nitrate buildup occurs at high elevation areas which have lots of agricultural activities and are the recharge zones for Kumamoto groundwater. It is therefore necessary to understand the infiltration mechanism in the unsaturated zone of these areas. Recently, unsaturated zone soil samples (down to 5 m depth) were collected at the slope of the western foot of Mt. Aso and the amount of recharge was estimated using oxygen and hydrogen isotope ratios of the water extracted from the soil (KUDO et al., 2016).

Research on the deep unsaturated zone (up to 15 m in depth) in Kumamoto using isotope tracers is still limited. The aim of this study is to augment the efforts in unsaturated zone studies in the Kumamoto region by trying to clarify the infiltration mechanism through estimation of the recharge amount and downward velocity of soil water using oxygen isotope ratios (water) in the recharge zone.

2. STUDY AREA

The Kumamoto region is about 1041 km^2 in area and bordered by the Chikushi-mountains to the North, the Mashiki-mountains to the South and the slope of the western foot of Mt. Aso to the East (Figure 1). There are three main rivers in the region; the Kikuchi, Shira and Midori Rivers which all flow into the Ariake Sea. The hydrogeological basement of the Kumamoto region consists of Mesozoic metamorphic and igneous rocks. The basement rocks are overlain by Quaternary pyroclastic flow deposits with high permeability (MIYOSHI et al., 2009). These deposits also cover the three major plateaus in the region which are the Kikuchi and Takayubaru plateaus to the east and the Ueki plateau to the North (Figure 1). They have altitudes of approximately 100 m. The unsaturated zone of these plateaus has a thickness of about 30 m. New volcanic ash layers are widely distributed on the top soil. The soil profiles of cores taken from the various sites studied are shown in Figure 2. Soil types include sandy clay, clay sand, volcanic ash sand, volcanic ash clay, gravelly clay, non-welded tuff and gravel. There are variations in soil type among the cores.

Groundwater in the Kumamoto region is recharged on the slope of Mt. Aso and around the plateaus, and flows from the northeastern part of the region to the southwest (TANIGUCHI et al., 2003). The aquifer formed by Quaternary pyroclastic flow deposits are divided into two main types by an aquiclude layer of lacustrine sediments; unconfined and confined aquifers (SHI-

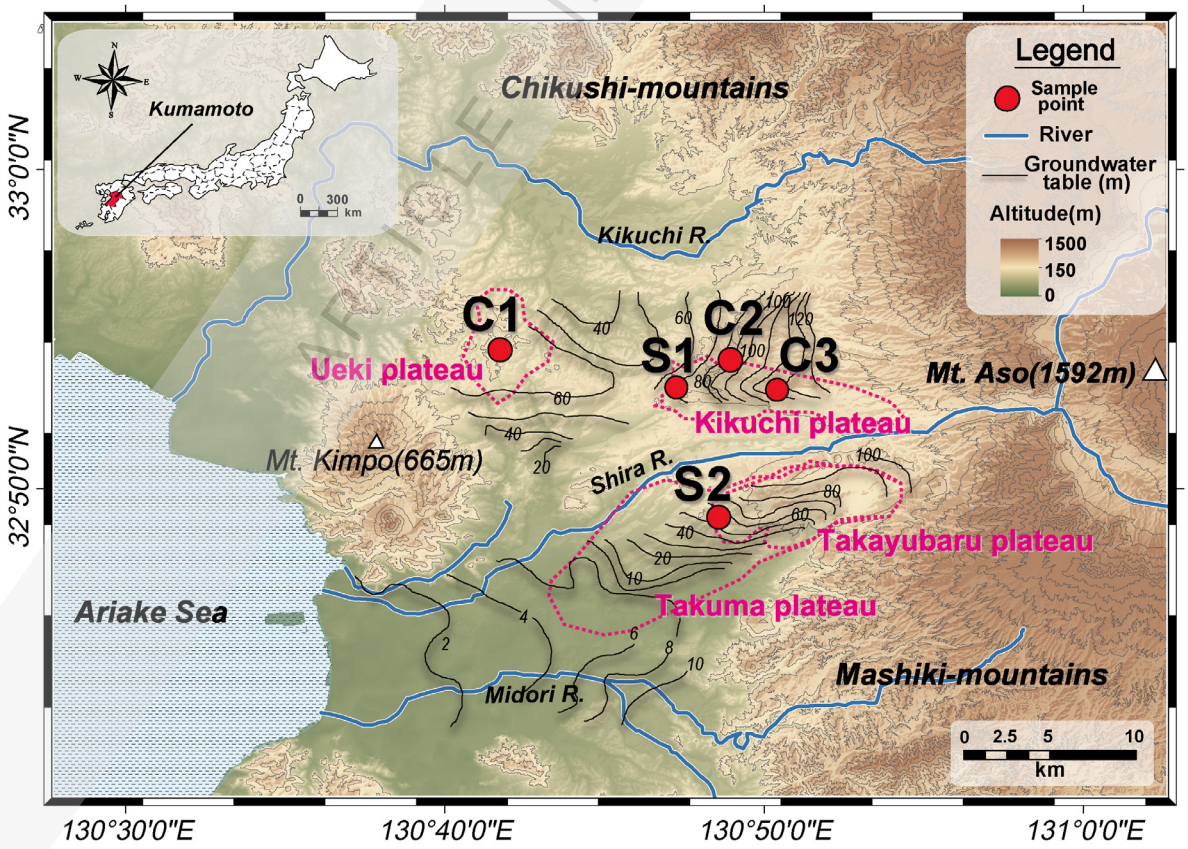

Figure 1. A map showing the Kumamoto region including sampling points. Red points show the drilling sites of the cores. The black lines and pink lines highlight the shallow groundwater table in the high-water season and the plateau areas.

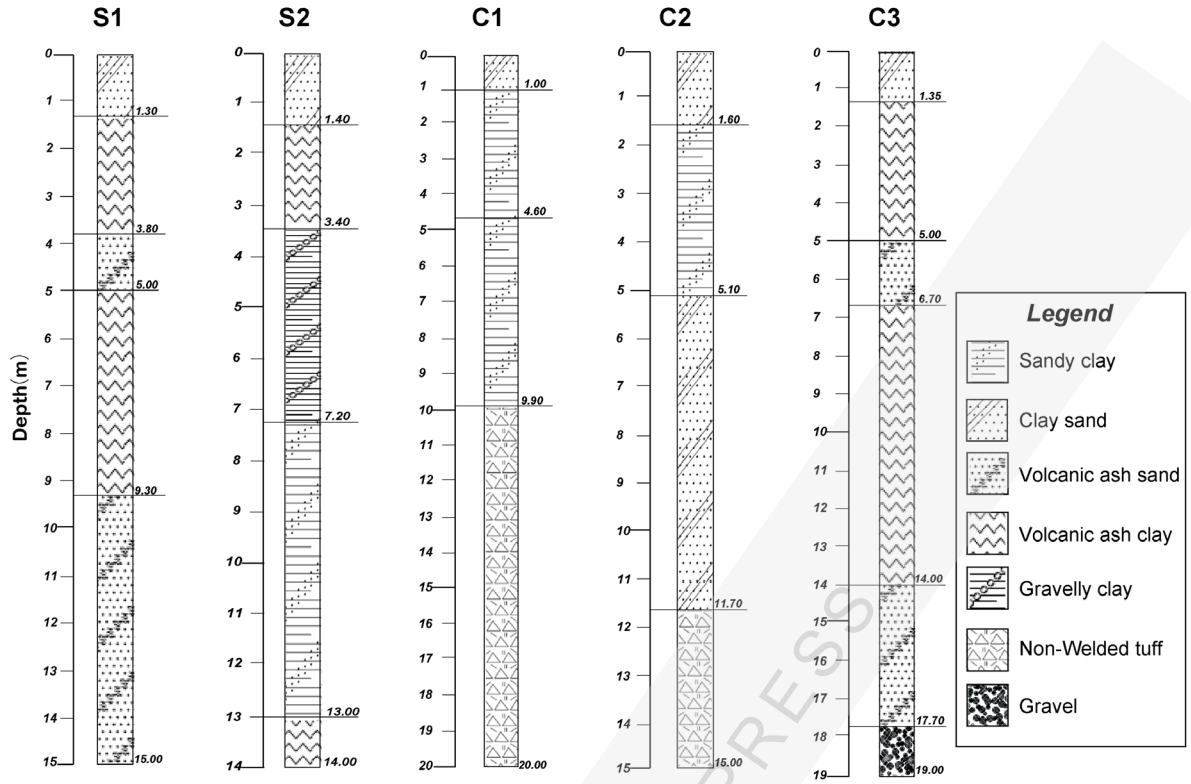

Figure 2. Soil profiles of drilled cores of the various sites.

MADA, 2012). The land-cover is 31% farmland, 29% forest and 11% paddy. The plateaus, which are groundwater recharge areas are mainly used as farmland. Average annual precipitation and temperature of Kumamoto from 1985 to 2015 are 1986 mm and 16.9 ˚C, respectively.

3. SAMPLING AND METHODS

In this study, 5 sampling sites were selected on the plateaus in the region (Figure 1). Each sampling site shows a different soil type, different fertilizer application method as well as treatment, different crops cultivated and different drilling times as shown in Table 1 and Figure 2. Core samples were taken from the unsaturated zone of each site using an excavator without adding water (ECO-3V, YBM, Japan).

The core was cut into 0.1 m samples and vacuum packed on-site to prevent evaporation of soil moisture before being taken to the laboratory for analysis. The 0.1 m fractions were split into two and each placed in a 100 cc sampling can. From one, soil water was centrifuged at pF 4.2 using centrifuge (MODEL SS-2200, SAKUMA, Japan) which spins for 2 hours. Although different for each depth, 2 to 20 ml of soil water was extracted. For the other sample, a three-phase meter that operates by Charles Boyle's law was used to measure the total volume of the liquid and solid phases after weighing (HORITA, 1985). The gas phase content (air within the pores) was obtained by subtracting the liquid and solid phase volumes from the total volume of the can.

Precipitation data used in this study was gathered at the Kumamoto University from Jan, 2005 to Jul, 2016. The data was acquired by sampling rainfall two to three times every month in a 2000 ml plastic bottle equipped with a funnel. A ping-pong ball was placed in the funnel to prevent evaporation. Samples were analyzed for hydrogen and oxygen isotope ratios. The results were converted to monthly data by evaluating the weighted average for each month.

Hydrogen and oxygen isotope ratios were measured by mass spectrometer (Delta-V, Thermo Fisher Scientific, USA). In the mass spectrometer, the gas achieved equilibrium with the oxygen and hydrogen isotopes of the water samples that were introduced.

Table 1. Details of sampling points. For the three-phase distribution, samples at 0.9 – 1.0 m, 5.0 – 5.1 m and 9.9 – 10.0 m are displayed. Details of all the water content data of the cores are shown in Table A1.

	Altitude(m)	Cultivated crop type	Drilling date	Depth (m)	Application status of fertilizers	Three- phase distribution (%)				Total soil water content (mm)		
							0.9 - 1.0 m	5.0 - 5.1 m	9.9 - 10.0 m	0 - 1.0 m	0 - 5.0 m	0 - 10 m
S1	98	corn for feed and Italian ryegrass	Nov-14	15	slurry and fertilizers	gas	9	14	45	580	2689	5331
						liquid	64	53	31			
						solid	27	33	24			
S2	67	corn for feed and Italian ryegrass	Nov-14	14	slurry and fertilizers	gas	29	1	25	501	2729	5036
						liquid	53	57	34			
						solid	18	42	41			
C1	105	vegetable	May-12	15	chemical fertilizers	gas	26	18	18	523	2345	4994
						liquid	55	52	47			
						solid	19	30	35			
C2	121	vegetable	May-12	15	chemical fertilizers	gas	27	17	16	540	3175	5729
						liquid	58	54	50			
						solid	15	29	34			
C3	137	carrot	Sep-15	10	manure and fertilizers	gas	26	12	5	536	3203	6249
						liquid	62	64	51			
						solid	12	24	44			

ARTICLE IN PRESS

Geologia Croatica

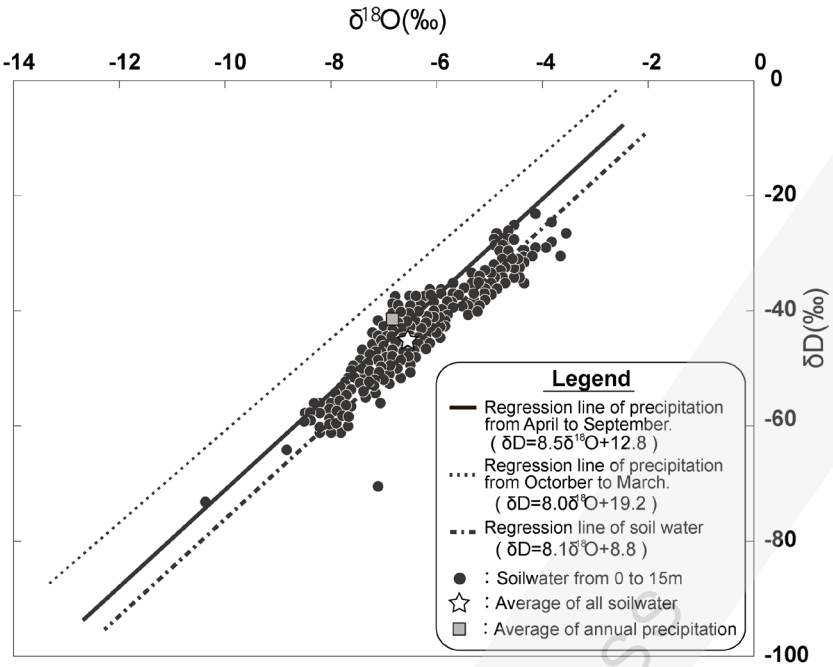

Figure 3. A plot diagram for $\delta^{18}O$ against δD of soil water samples.

The hydrogen and oxygen isotopes are expressed as relative differences (δ values) from Standard Mean Ocean Water in per mil (‰). The accuracy of the measured value was within ± 0.50‰ for δD and within ± 0.05‰ for $\delta^{18}O$.

4. RESULTS

Plots of δD and $\delta^{18}O$ for all precipitation and soil water samples are shown in Figure 3. The elevation effect on water isotopes was evaluated. The maximum elevation difference between the cores was calculated to be 70 m. This elevation effect on the hydrogen isotope in the study area is reported as -0.027‰ per metre (KAGABU et al., 2017). Hence, the maximum elevation effect of the sampling points is about 1.9‰. However, it can be seen from Figure 3 that all plots of δD and $\delta^{18}O$ fall along the summer Local Meteoric Water Line (April to September) regardless of elevation effect. Therefore, it was not considered in our estimations. The isotope ratios of precipitation for 11 years (2005 to 2015) were divided into two groups depending on season; summer (April to September) and winter (October to March). The slopes of the regression lines of the summer and winter data are 8.5 ($r^2 = 0.87$, $p < 0.0001$, $n = 70$) and 8.0 ($r^2 = 0.84$, $p < 0.0001$, $n = 65$) respectively, which are almost equal to 8, the slope of the World Meteoric Water Line (CRAIG, 1961).

However, the intercept of the regression line for summer and winter data are 12.8 and 19.2, respectively. The intercept for all soil water was 8.8 ($r^2 = 0.83$, $p < 0.01$, $n = 566$) which was rela-

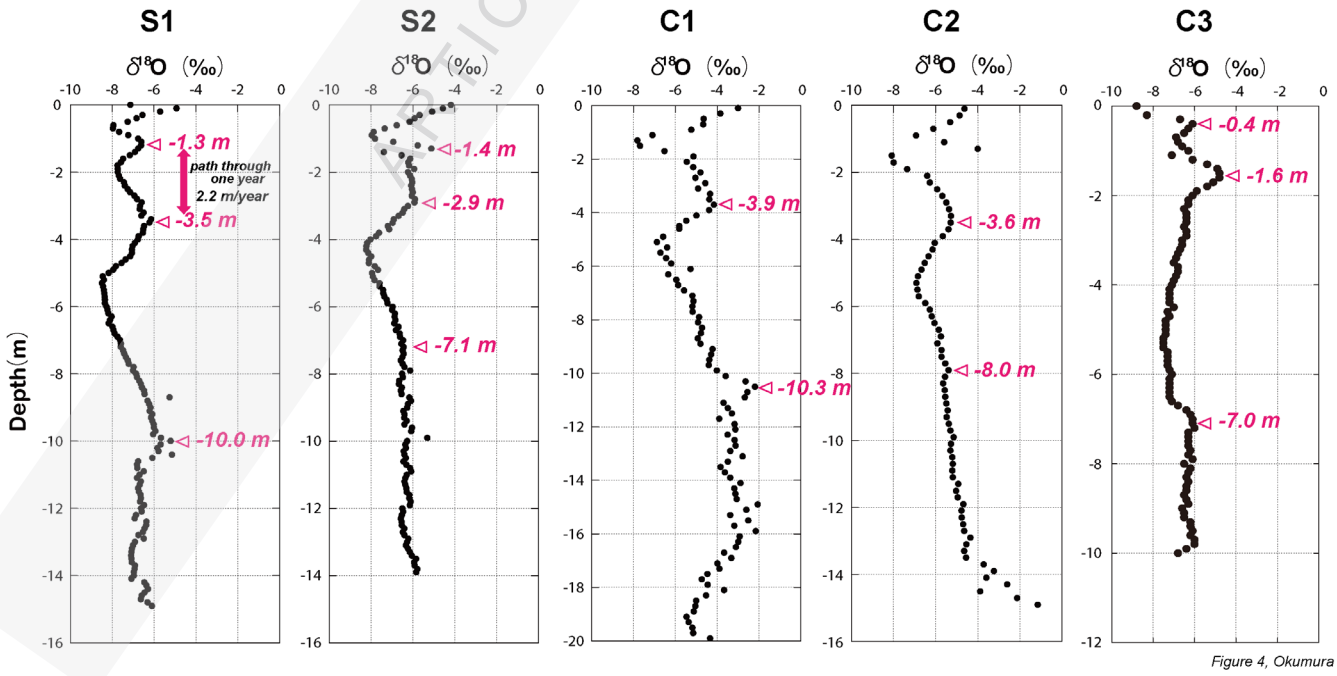

Figure 4. Oxygen stable isotope ratio vertical profile diagrams for each core. Triangle marks show peak depth with a relatively high isotope ratio.

tively close to the intercept for summer (Figure 3). Moreover, the averages of δD and $\delta^{18}O$ of soil water samples were -41.3‰ and -6.7‰, respectively which are similar to the isotopic composition for summer precipitation (δD = -45‰, $\delta^{18}O$ = -7‰) compared with that of winter ($\delta^{18}O$ = -5‰ δD = -32‰). Evaporation occurring in the soil is generally considered to be non-equilibrium evaporation, in which case the slope of a regression line in the soil water tends to be smaller ranging from 2 to 5 (BARNES & TURNER, 1998; CLARK & FRITZ, 1997). In this study, the slope for all soil water sample plots was 8.1 ($r^2 = 0.83$, $p < 0.01$, n = 566), which implies evaporation in the top soil was not considerable.

Figure 4. shows the vertical profiles of $\delta^{18}O$ in soil water. These profiles display several relatively high isotopic composition peaks, e.g., at depths of 1.2 m and 3.5 m for the S1 core. It is interpreted that the vertical change of $\delta^{18}O$ is reflective of the seasonal isotopic composition of the recharging precipitation which is high in summer and low in winter. These peaks hold the seasonal information of precipitation.

The plots in Figure 4. show that it takes one year for new peaks to appear on the profile. It can be inferred from the S1 core profile that the infiltration rate in the top 3.5 m would be 2.2 m/yr approximately. The next peak after 3.5 m is at 10 m depth. Therefore, the depth interval from peak to peak is observed to be increasing. Moreover, there is a gradual change in peak compared with the peak at 3.5 m depth. The profiles of the other cores show similar characteristic peaks. It is assumed that as soil water infiltrates deeper, the more dispersion may occur when the peaks are averaged. Therefore, there is a limit to understanding the infiltration rate from the peak position.

Table 1. shows the liquid and solid phases at depths of 1 m, 5 m and 10 m for each core. In all cores, the solid phase varies between 15% and 27% at 1 m depth, while porosity ranges between 73 and 88%. According to SHIMOZU (1986), Mt. Aso volcanic ash soil porosity ranges from approximately 70 to 90%. Hence, the sampling points have the characteristics of volcanic ash soil. The S1 liquid at 10 m depth is small compared with other cores. On the other hand, in C3, the liquid phase occupies 96% of the pore volume at a depth of 10 m. In particular, C3 has a high liquid phase at all depths. Therefore, C3 soil is considered to have a relatively high water holding capacity. It is important to determine the recharge rate and downward velocity of soil water by incorporating a water content profile.

5. DISCUSSION

In order to estimate the average downward velocity of soil water from 0–15 m depth using stable isotope ratios, the isotope profile of soil water was compared with the model isotope profile of the monthly infiltration amount obtained by subtracting evapotranspiration from precipitation. In building the model profile based on precipitation, the time-series data of precipitation was converted into depth data. To do this, the Displacement Flow Model (DFM) proposed by Anderson and SEVEL (1974) was applied. DFM was used earlier by SHIMADA (1988) and KUDO et al. (2016) to understand the behaviour of water in the unsaturated zone. The model assumes a piston flow. Here, a piston flow is also assumed in an attempt to estimate the recharge rates and the downward velocity.

The methods used to calculate DFM are described below. Equation (1) which is the water balance equation was used to estimate Infiltration (I) into the ground.

$$I = P\text{-}R\text{-}E \quad (1)$$

Where P, R and E are amounts of precipitation, runoff and evapotranspiration, respectively. In estimating E, Equation (2) was used. This is a modified form of Thornthwaite's equation (THORNTHWAITE, 1948) used to handle wide temperature ranges. This is based on the principle that the amounts of precipitation and evapotranspiration are directly proportional to the atmospheric pressure (TAKAHASHI, 1979).

$$E(T) = \frac{3100\,P}{3100 + 1.8\,P^2 \exp\left(-\frac{34.4\,T}{235 + T}\right)} \quad (2)$$

Where T is monthly temperature, P is monthly precipitation.

Here, R in equation (1) was replaced with αP by setting the direct runoff coefficient α, assuming that a constant rate of P directly flows out. α was varied from 0 to 0.3 at an interval of 0.02 with reference to Kudo et al. (2016), and the highest coefficient of determination between the actual profile and the modeled profile was selected. The fraction of monthly precipitation used for each depth was determined to successively represent infiltration from the surface which corresponds to the soil water content. Based on the fraction of the monthly precipitation for each depth, weighted averages of the oxygen isotope ratios in precipitation were estimated to create a model isotope vertical profile (TSUJIMURA et al., 1994).

DFM was used to create a depth profile by applying the time variation of the tracer concentration. The downward velocity of soil water and recharge rate were estimated based on the depth-time information obtained when the profile was created using DFM. Monthly temperature and precipitation data for Kumamoto City collected by the Japan Meteorological Agency were used in the DFM. Time series data used in the DFM calculations are shown in Figure 5 and include precipitation, evapotranspiration, temperature and $\delta^{18}O$ in precipitation.

The profile of $\delta^{18}O$ in soil water and that of the modeled profile by DFM are shown in Figure 6. The coefficient of determination (r^2) between the measured $\delta^{18}O$ and modeled $\delta^{18}O$ by DFM was lower than 0.5 for all cores (black line vs gray line in Figure 6). This indicates that direct results by DFM could not trace the behaviour of measured $\delta^{18}O$ profile successfully. This may be due to the fact that input precipitation $\delta^{18}O$ data are based on a weighted average of several precipitation events and did not cover precisely all actual precipitation $\delta^{18}O$ records. Moreover, the concept of the DFM model might be the other reason which does not account for dispersion phenomena. To solve this problem, variance due to these factors was considered by calculating moving averages of DFM values and the condition that resulted in the highest correlation between measured $\delta^{18}O$ and modeled $\delta^{18}O$ was employed (KUDO et al., 2016). Consequently, we found the best condition resulting in the highest correlation between measured $\delta^{18}O$ and modeled $\delta^{18}O$ (moving average DFM), as shown by the black and dotted lines in Figure 6. The coefficient of determination for all cores was ($r^2 > 0.8$, $p < 0.02$), suggesting that our DFM approach satisfactorily reflects water behaviour at the studied sites.

The estimated result for each site is shown in Table 2. In S1, it was observed that the downward velocity was the highest of all the sites. This is because the soil has a low liquid phase around 10 m depth. Comparing C3 and S1 which have the same soil type, S1 has a higher recharge rate and velocity. This may be due to the

ARTICLE IN PRESS

Geologia Croatica

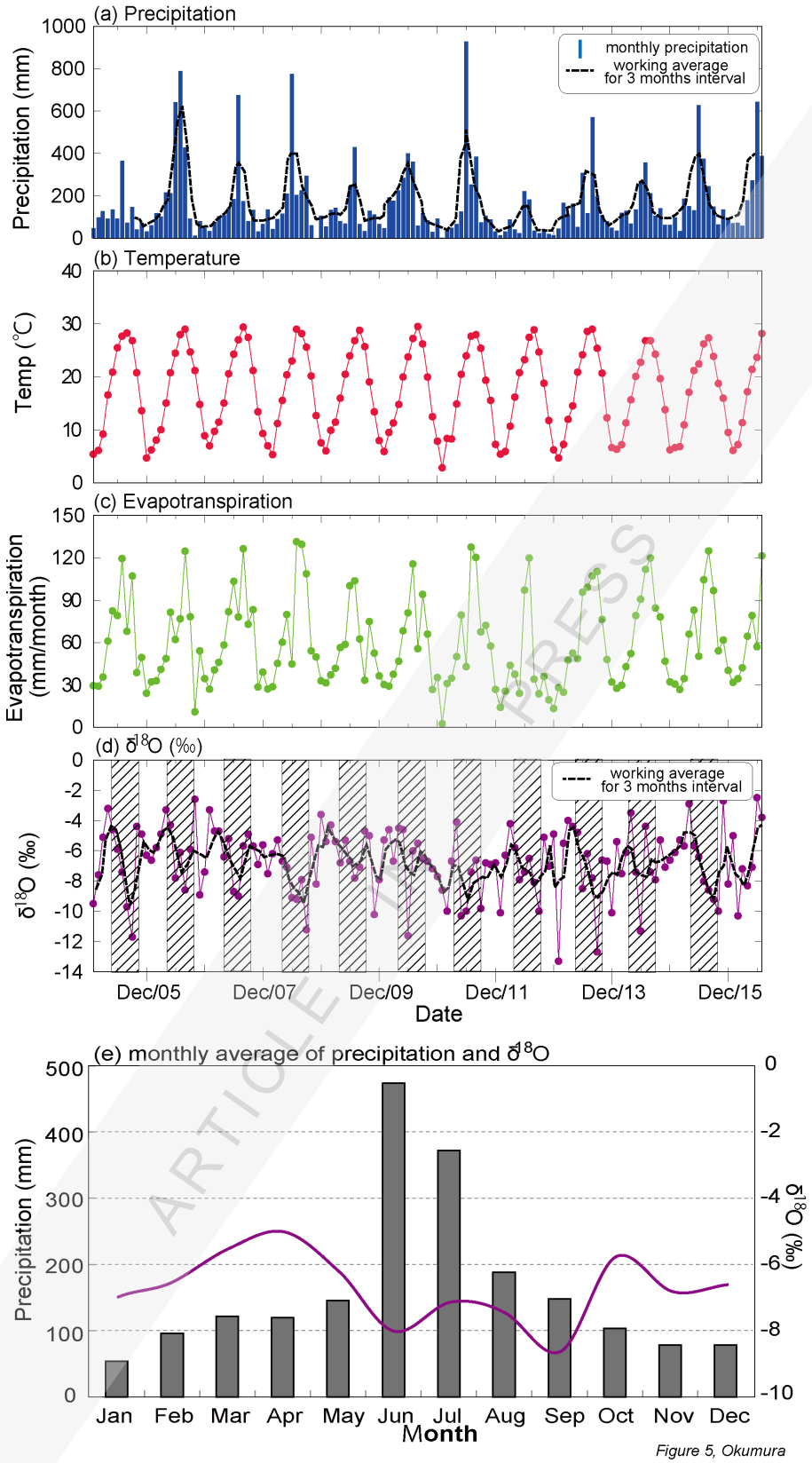

Figure 5. Time series distribution of (a) Precipitation (b) Temperature (c) Evapotranspiration (d) Oxygen isotope ratio in precipitation (e) Monthly average of precipitation (bar graph) and oxygen isotope ratio (line graph) from 2005 to 2015. The dotted lines in (a) and (d) represent the moving average of 3 month data. The hatched area in (d) represents the summer season (April – September).

difference in soil conditions. For C3 and S2, it can be seen that the downward velocity of C3 is relatively lower, even though the recharge rate is higher. The most likely reason is that, C3 soil has the highest water content (Table 1). Therefore, it is evident that the difference in the average recharge rate and downward velocity for each core is due to the difference in soil conditions such as soil type and water content at each core depth (Table 1 and Figure 2).

Geologia Croatica

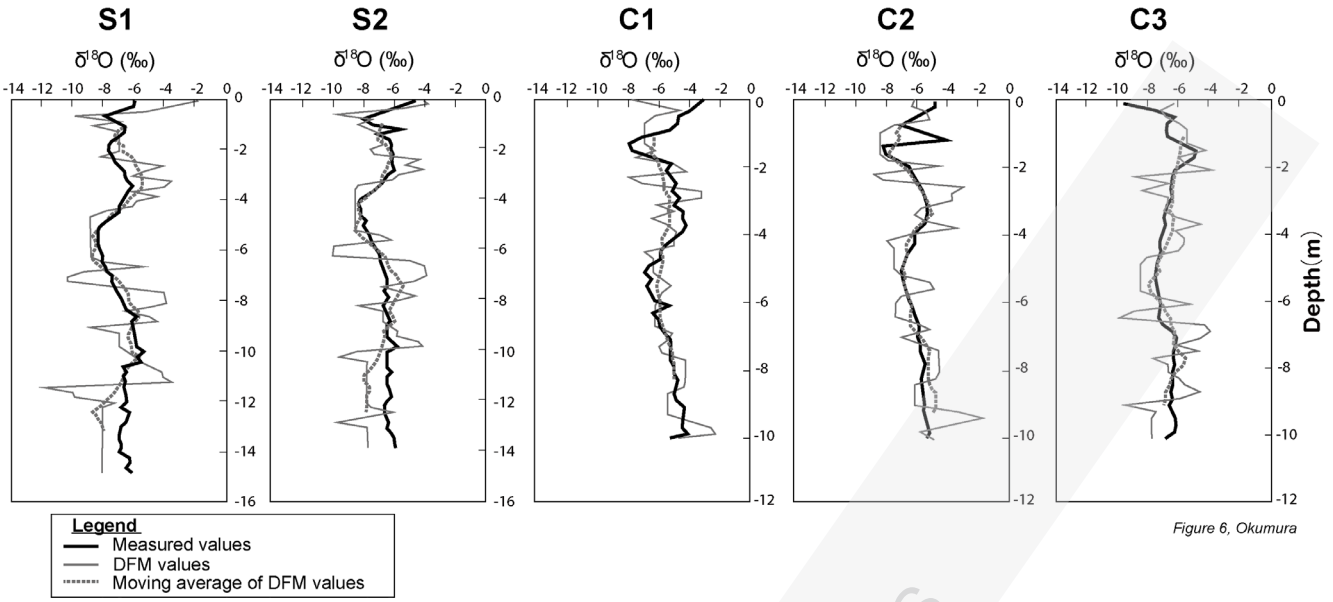

Figure 6, Okumura

Figure 6. The profile of measured $\delta^{18}O$ values in soil water (black line), DFM (gray line) and the moving average of DFM (dotted line).

Although there are regional differences, the annual average recharge rate in the recharge area of the plateau was estimated to range from 745 to 1058 mm/yr, and the annual average downward velocity from 1.37 to 2.34 m/yr. Furthermore, the average recharge rate and average downward velocity calculated from the estimation results in Table 2 for S1, C2 and C3 in the northeastern recharge area (Figure 1) are 893 mm/yr and 1.7 m/yr, respectively. These somehow match the recharge amount of 1137 mm/yr and infiltration rate of 2.3 m/yr of the Kumamoto region estimated using tritium (SHIMADA & UENO, 2016). However, our estimated value was smaller than that of SHIMADA & UENO (2016). The difference may be due to regional heterogeneities.

In estimating the infiltration time for water to reach the aquifers, the unsaturated zone thickness was divided by the downward velocity as shown in Table 2. The unsaturated zone thickness was obtained by subtracting the groundwater level elevation in the lowest water level period at the sampling points from the ground surface elevation. The transportation time from the ground surface to the aquifer was estimated to range from 9 to 24 years. KAGABU et al. (2017) estimated the ages of groundwater in the recharge zone at Kikuchi plateau using ^{85}Kr age tracer to range from 15 to 25 years (n = 3). Although different sample points were selected in this study, the water transportation time from the surface to the aquifer estimated by DFM is equivalent to the recharge area's groundwater ages calculated by KAGABU et al., (2017). Therefore, it can be reliably concluded that soil water reaches the aquifer over a period of about 9 to 25 years in the main recharge area of the Kumamoto region.

6. CONCLUSION

The recharge rate and downward velocity in the unsaturated zone of the recharge area of the Kumamoto region were estimated for 5 soil cores using oxygen isotope ratios in soil water as a tracer. Consequently, the annual average recharge rate was estimated to range from 745 to 1058 mm/yr, and the annual average downward velocity from 1.37 to 2.34 m/yr. Differences in the estimated recharge rate and downward movement velocity are due to the variation in soil properties of each site. Water transportation time from the surface to the aquifers was estimated to be 9 to 24 years, corresponding well to groundwater ages in the same recharge area. With the assumption that nitrogen loaded on the surface will be transported with soil water, nitrate should leach to the aquifer in 9 to 24 years once fertilizers and manures are applied. Such information is primarily important for the management and preservation of groundwater resources. However, nitrate transportation and behaviour in the unsaturated zone should be affected by diffusion, microbial activities, etc. The results of this study therefore may not be able to fully account for the transportation of solutes through the unsaturated zone to the aquifers. To better understand nitrate infiltration characteristics, it is necessary to promote future studies on nitrate concentrations and isotope ratios to aid further understanding of soil water infiltration mechanisms.

ACKNOWLEDGMENT

We thank Mr. Satoshi SAKAEDA of the Kumamoto Prefectural Government for his help during the field surveys. We also thank Associate Prof. Kimpei ICHIYANAGI, Graduate School of Sci-

Table 2. Infiltration time and velocity of studied cores estimated using DFM. The thickness of the unsaturated zone is estimated using shallow groundwater level distribution.

	S1	S2	C1	C2	C3
Annual average of recharge rates (mm/yr)	1058	846	745	795	869
Annual average of downward velocity (m/yr)	2.34	1.68	1.46	1.38	1.37
Thickness of unsaturated layer (m)	30	15	33	33	19
Average water transportation time from surface reaching to aquifer (yr)	13	9	23	24	14

Geologia Croatica

ence and Technology of Kumamoto University for his support with rainfall sampling. We express our gratitude to Ms. Miho MASAKI for making available her soil profile data set for this work. Finally, we wish to thank the farmers who readily made available their fields for this study. This study was funded by Commissioned Research of Kumamoto Prefectural Government.

REFERENCES

ANDERSEN, L. J. & SEVEL, T. (1974): Six Years Environmental Tritium Profiles in the Unsaturated Zones, Gronhoj, Denmark.– Isotope Techniques in Groundwater Hydrology, IAEA Vienna, 1, 3–20.

BAHARATI, L., LEE, K.H., ISENHART, T.M. & SCHULTZ, R.C. (2002): Soil-water Infiltration Under Crops, Pastures, and Established Riparian Buffer in Midwestern USA.– Agroforestry Systems, 56, 249–257.

BARNES, C. & ALLISON, G.B. (1983): The Distribution of Deuterium and ^{18}O in Dry Soils, 1 Theory.– Journal of Hydrology, 60, 141–156.

BARNES, C.J. & TURNER, J.V. (1998): Isotopic Exchange in Soil Water – Isotope Tracers.– In: KENDALL, C. & MCDONNELL, J.J. (eds.): Catchment Hydrology, Elsevier Amesterdam, 137–163.

BARTH, S.R. (2000): Stable isotope geochemistry of sediment-hosted groundwater from a Late Paleozoic-Early Mesozoic section in central Europe.– Journal of Hydrology, 235, 72–87.

BEVEN, K. & GERMANN, P. (1982): Macropores and Water Flow in Soils.– Water Resources Research, 18, 1311–1325.

CLARK, I. & FRITZ, P. (1997): Groundwater – Environmental Isotopes in Hydrogeology.– CRC Press/Lewis Publishers, 85–89.

CLOUTIER, V., LEFEBVRE, R., THERRIEN, R & Savard, M.M. (2008): Multivariate statistical analysis of geochemical data as indicative of the hydrogeochemical evolution of groundwater in sedimentary rock aquifer system.– Journal of Hydrology, 353, 294–313.

CRAIG, H. (1961): Isotope Variations in Meteoric Waters.– Science, 133, 1702–1703.

De VRIES, J.J., SELAOLO, E.T. & BEEKMAN, H.E. (2000): Groundwater Recharge in the Kalahari, with Reference to Paleo-hydrologic Conditions.– Journal of Hydrology, 238, 110–123.

DELIN, G.N. & HERKELRATH, W.N. (2017): Effects of crude oil on water and tracer movement in the unsaturated and saturated zones.– Journal of Contaminant Hydrology, 200, 49–59.

DEMLIE, M., WOHNLICH, S., WISOTZKY, F. & GIZAW, B. (2007): Groundwater recharge, flow and hydrogeochemical evolution in a complex volcanic aquifer system, central Ethiopia.– Hydrogeology Journal, 15, 1169–1181.

GUYMON, G.L. (1994): Preface and Introduction – Unsaturated Zone Hydrology.– P.T.R. Prentice Hall, 1–6.

HARRIS, R.C. (2000): Tritium as a tracer of groundwater sources and movement in the Safford Basin, Graham County, Arizona.– Arizona Geological Survey, 9, 1–56.

HORITA, Y. (1985): The Measurement of Physical Soil by the Actual Volume.– Research of forest in Kyusyu, 38, 139–141 (in Japanese).

HOSONO, T., TOKUNAGA, T., KAGABU, M., NAKATA, H., ORISHIKIDA, T., LIN, I.T. & SHIMADA, J. (2013): The Use of $\delta^{15}N$ and $\delta^{18}O$ Tracers with an Understanding of Groundwater Flow Dynamics for Evaluating the Origins and Attenuation Mechanisms of Nitrate Pollution.– Water Research, 47, 2661–2675.

HOSONO, T., TOKUNAGA, T., TSUSHIMA, A. & SHIMADA, J. (2014): Combined use of $\delta^{13}C$, $\delta^{15}N$, and $\delta^{34}S$ tracers to study anaerobic bacterial processes in groundwater flow systems.– Water Research, 54, 284–296.

HEM, J.D. (1985): Study and Interruption of the Chemical Characteristics of Natural Water.– United States Geological Survey Water-Supply Paper, 2254, 174–180.

JOHNSTORN, G.T., COOK, P.G., FRAPE, S.K., PLUMMER, L.N., BUSENBERG, E, & BLACKPORT, R.J. (1998): Groundwater age and nitrate distribution within a glacial aquifer beneath a thick unsaturated zone.– Ground Water, 36, 171–180.

KAYANE, T., TANAKA, T. & SHIMADA, J. (1980): The Transportation of Soil Water in Kanto Loam Formation Using Environmental Tritium as a Tracer.– Geographical Review of Japan, 53–4, 225–237 (in Japanese).

KABEYA, N., OHTE, N., SUGIMOTO, A., YOSHIKAWA, K. & WANG, L. (2002): Effects of the Ground Cover Conditions on Horizontal Profiles of Chloride Concentration, Oxygen and Hydrogen Stable Isotope Ratios of Groundwater in Mu Us Desert, China.– Journal of Japan Society of Hydrology and Water Resources, 15, 13–22 (in Japanese with English Abstract).

KAGABU, M., MATSUNAGA, M., IDE, K., MOMOSHIMA, N. & SHIMADA, J. (2017): Groundwater Age Determination Using ^{85}Kr and Multiple Age Tracers (SF_6, CFCs and ^3H) to Elucidate Regional Groundwater Flow Systems.– Journal of Hydrology, Regional Studies, 12, 165–180.

KUDO, K., SHIMADA, J., MARUYAMA, A. & TANAKA N. (2016): The Quantitative Evaluation of Groundwater Recharge Rate Using Displacement Flow Model with Stable Isotope Ratio in the Soil Water of Different Vegetation Cover.– Journal of Japan association of Groundwater Hydrology, 58, 31–45 (in Japanese with English Abstract).

LIN, R. & WEI, K. (2006): Tritium profiles of pore water in the Chinese loess unsaturated zone: Implications for estimation of groundwater recharge.– Journal of Hydrology, 328, 192–199.

MAHARA, Y. (1995): Noble Gases Dissolved in Groundwater in a Volcanic Aquifer: Helium Isotopes in Kumamoto Plain.– Environmental Geology, 25, 214–224.

MIYAGIMA, T. & NAGATA, S. (2008): The Stable Isotope and the Evaluation of Watershed Environment.– The Academic Publisher in Kyoto University, Japan, 59–65 (in Japanese).

MIYOSHI, M., FURUKAWA, K., SHINMURA, T., SHIMONO, M. & HASENAKA, T. (2009): Petrography and Whole-rock Geochemistry of Pre-Aso Lavas from the Caldera Wall of Aso Volcano, Central Kyusyu.– Journal of the Geological Society of Japan, 115, 672–687. (in Japanese with English Abstract).

NICHOL, C., SMITH, L. & BECKIE, R. (2005): Field-scale experiments of unsaturated flow and solute transport in a heterogeneous porous medium.– Water Resour. Res., 41/5, W05018.

NIMMO, J.R. (2007): Simple predictions of maximum transport rate in unsaturated soil and rock.– Water Resour. Res., 43/5, http://onlinelibrary.wiley.com/doi/10.1029/2006WR005372/pdf.

RUSSELL, E.W. (1973): Soil Conditions and Plant Growth.– 10th ed., Longman, London.

SHIMADA, J. (1988): The Mechanism of Unsaturated Flow through a Volcanic Ash Layer under Humid Climatic Conditions.– Hydrological Processes, 2, 43–59.

SHIMADA, J. (2012): Sustainable Management of Groundwater Resources for 700.000-Plus Residents: A Practional Example of the Transboundary Management of Groundwater Resources in the Kumamoto Area, Japan. The Dilemma of Boundaries. TANIGUCHI, M. & SHIRAIWA, T. (eds.) Springer Japan, 235–246.

SHIMADA, J. & UENO, M. (2016): The Challenge to Sustainable Groundwater Use.– Seibundo, 8, 144–151 (in Japanese).

SHIMOZU, M. (1986): On the Characteristics of groundwater in the Hydrologic Cycle of the Aso Volcano.– Journal of Japan Association of Groundwater Hydrology, 28, 1–13.

SPALDING, R.F., EXNER, M.E., LINDAU, C.W. & EATON, D.W. (1982): Investigation of source of groundwater nitrate contamination in Burbank-Wallula area of Washington, U.S.A.– Journal of Hydrology, 58, 307–324.

TAKAHASHI, K. (1979): Expression to estimate evapotranspiration using monthly average temperature and monthly precipitation.– Journal of Meteorological Society of Japan, 26, 29–32 (in Japanese).

TANIGUCHI, M., SHIMADA, J. & UEMURA, T. (2003): Transient effects of surface temperature and groundwater flow on subsurface temperature in Kumamoto Plain, Japan.– Physics and Chemistry of the Earth, 28, 477–486.

THORNTHWAITE, C.W. (1948): An approach toward a rational classification of climate.–Geographical Review, 38, 55–94.

TOMIIE, K., IWASA, Y., MAEDA, K., OTSUZUKI, M., YUNOUE, T., KAKIMOTO, R. & KAWAGOSHI, Y. (2009): Present Status and Feature of Groundwater Contamination by Nitrate-nitrogen in Kumamoto City.– Journal of Water and Environment Technology, 7, 19–28.

TSUJIMURA, M. (1994): Dynamic Behaviour of Soil Water Movement in a Headwater Basin.– Unpubl. Ph.D Thesis, University of Tsukuba, Japan, 132 p.

TSUJIMURA, M. & TANAKA, T. (1998): Evaluation of Evaporation Rate from Forested Soil Surface Using Stable Isotopic Composition of Soil Water in a Headwater Basin.– Hydrological Processes, 12, 2093–2103.

UMEZAWA, Y., HOSONO, T., ONODERA, S., SIRINGAN, F., BUAPENG, S., DELINOM, R., YOSHIMIZU, C., TAYASU, I., NAGATA, T. & TANIGUCHI, M. (2008): Source of nitrate and ammonium contamination in groundwater under developing Asian megacities.– Science of the Total Environment, 404, 361–376.

YABUSAKI, S., TASE, N. & SHIMADA, J. (2011): Vertical Profile of Stable Isotopes in Soil Water through the Volcanic Ash Soil Layer in Japan.– The Earth Environmental Research, 13, 43–57 (in Japanese with English Abstract).

ZHANG, Y., LI, F., ZHANG, Q., LI, J. & LIU, Q. (2014): Tracing nitrate pollution sources and transportation in surface- and ground-waters using environmental isotopes.– Science of Total Environment, 490, 213–222.

ZIMMERMANN, U., EHHALT, D., MUNNICH, K.O., ROETHER, W., KREUTZ, W., SCHUBACH, K. & SIRGEL, O. (1966): Using Tracers to Determine Movement of Soil Moisture and Evapotranspiration.– Science, 152, 346–347.

LAND USE CONTROL BACK-UP SYSTEM (May 11, 2017). Land Use Control back-up System, Retrieved from http://lucky.tochi.mlit.go.jp/

JAPAN METEOROLOGICAL AGENCY (March 20, 2018), Past climate data, Retrieved from http://www.data.jma.go.jp/gmd/risk/obsdl/index.php

IN PRINT

APPENDIX

Table A1 Isotope composition of soil water in each core

	S1 core			S2 core			C3 core		
depth (m)	δD (‰)	$\delta^{18}O$ (‰)	d-excess (‰)	δD (‰)	$\delta^{18}O$ (‰)	d-excess (‰)	δD (‰)	$\delta^{18}O$ (‰)	d-excess (‰)
0.0 - 0.1	-42.1	-7.13	14.94	-23.5	-4.18	9.95	-64.1	-8.84	6.61
0.1- 0.2	-27.9	-4.93	11.54	-25.8	-4.57	10.79	-72.8	-10.35	10.07
0.2 - 0.3	-36.3	-5.71	9.38	-33.6	-5.08	7.03	-56.2	-8.34	10.53
0.3 - 0.4	-42.2	-6.55	10.20	-38.7	-5.69	6.87	-44.3	-6.66	9.00
0.4 - 0.5	-45.3	-6.84	9.42	-41.2	-5.91	6.11	-42.8	-6.09	5.91
0.5 - 0.6	-50.0	-7.27	8.16	-45.82	-6.16	3.43	-45.8	-6.35	5.03
0.6 - 0.7	-56.5	-7.94	7.02	-50.2	-6.77	3.99	-47.4	-6.48	4.43
0.7 - 0.8	-56.7	-7.97	7.06	-55.2	-7.36	3.69	-48.7	-6.90	6.46
0.8 - 0.9	-54.1	-7.67	7.26	-59.9	-7.88	3.15	-47.3	-6.84	7.36
0.9 - 1.0	-50.8	-7.24	7.12	-61.0	-7.97	2.77	-45.0	-6.64	8.11
1.0 - 1.1	-47.0	-6.76	7.08	-59.0	-7.82	3.53	-41.9	-6.29	8.34
1.1 - 1.2	-46.4	-6.61	6.48	-52.1	-6.95	3.51	-70.5	-7.09	-13.80
1.2 - 1.3	-45.9	-6.63	7.14	-41.1	-5.77	5.04	-39.1	-6.07	9.45
1.3 - 1.4	-46.6	-6.76	7.48	-33.6	-5.12	7.34	-33.8	-5.40	9.45
1.4 - 1.5	-48.1	-6.92	7.26	-50.3	-7.39	8.87	-29.5	-4.87	9.45
1.5 -1.6	-49.4	-7.16	7.88	-44.5	-6.54	7.84	-29.5	-4.76	8.55
1.6 - 1.7	-53.0	-7.48	6.84	-36.7	-6.13	12.28	-31.0	-4.80	7.36
1.7 - 1.8	-53.6	-7.59	7.12	-38.1	-6.22	11.65	-33.9	-5.09	6.80
1.8 - 1.9	-54.1	-7.75	7.90	-42.1	-6.19	7.43	-35.3	-5.38	7.75
1.9 - 2.0	-53.8	-7.74	8.12	-44.5	-5.95	3.12	-38.6	-5.86	8.25
2.0 - 2.1	-52.8	-7.74	9.12	-44.5	-6.24	5.37	-41.5	-6.12	7.47
2.1 - 2.2	-52.1	-7.69	9.42	-43.1	-6.13	5.92	-43.3	-6.32	7.23
2.2 - 2.3	-50.8	-7.62	10.16	-43.4	-6.06	5.01	-43.2	-6.34	7.49
2.3 - 2.4	-48.7	-7.44	10.82	-43.9	-6.03	4.28	-44.2	-6.47	7.54
2.4 - 2.5	-47.5	-7.40	11.70	-43.8	-6.08	4.82	-43.6	-6.38	7.42
2.5 - 2.6	-46.5	-7.27	11.66	-43.5	-6.05	4.97	-43.9	-6.44	7.56
2.6 - 2.7	-44.8	-7.15	12.40	-43.7	-6.00	4.33	-44.2	-6.42	7.17
2.7 - 2.8	-43.3	-6.94	12.22	-43.3	-6.06	5.14	-44.8	-6.45	6.80
2.8 - 2.9	-41.8	-6.81	12.68	-43.2	-5.90	4.06	-44.6	-6.44	6.90
2.9 - 3.0	-41.7	-6.60	11.10	-44.0	-5.93	3.48	-44.7	-6.38	6.37
3.0 - 3.1	-41.3	-6.67	12.06	-46.8	-6.23	3.05	-45.6	-6.64	7.51
3.1 - 3.2	-40.6	-6.68	12.84	-48.3	-6.42	3.05	-45.8	-6.61	7.16
3.2 - 3.3	-40.3	-6.51	11.78	-49.6	-6.50	2.42	-46.7	-6.74	7.17
3.3 - 3.4	-40.8	-6.61	12.08	-51.7	-6.69	1.89	-47.0	-6.82	7.61
3.4 - 3.5	-43.5	-6.15	5.70	-52.9	-6.91	2.40	-48.0	-6.89	7.10
3.5 - 3.6	-44.8	-6.22	4.96	-52.4	-6.97	3.30	-48.4	-6.96	7.30
3.6 - 3.7	-46.4	-6.48	5.44	-51.9	-7.20	5.63	-47.2	-6.78	7.05
3.7 - 3.8	-47.5	-6.52	4.66	-54.3	-7.14	2.77	-48.4	-6.81	6.07
3.8 - 3.9	-47.9	-6.53	4.34	-56.7	-7.62	4.22	-49.0	-6.93	6.43
3.9 - 4.0	-49.0	-6.74	4.92	-57.8	-7.76	4.26	-49.4	-6.97	6.34
4.0 - 4.1	-49.3	-6.77	4.86	-60.0	-8.03	4.30	-50.8	-7.09	5.88
4.1 - 4.2	-49.6	-6.92	5.76	-60.3	-8.19	5.27	-51.9	-7.20	5.68
4.2 - 4.3	-49.9	-7.03	6.34	-61.3	-8.22	4.47	-52.3	-7.15	4.91
4.3 - 4.4	-50.0	-7.06	6.48	-60.8	-8.24	5.06	-52.5	-7.21	5.17
4.4 - 4.5	-50.0	-7.06	6.48	-60.6	-8.14	4.48	-52.8	-7.23	5.00
4.5 - 4.6	-50.4	-7.15	6.80	-59.7	-8.00	4.28	-51.7	-6.99	4.21
4.6 - 4.7	-51.6	-7.37	7.36	-59.9	-8.09	4.84	-53.1	-7.29	5.19
4.7 - 4.8	-52.5	-7.56	7.98	-60.2	-8.11	4.71	-52.7	-7.18	4.77
4.8 - 4.9	-53.8	-7.83	8.84	-58.4	-7.83	4.26	-53.2	-7.35	5.64
4.9 - 5.0	-54.9	-7.96	8.78	-56.7	-7.67	4.69	-53.20	-7.39	5.95
5.0 - 5.1	-57.2	-8.18	8.24	-57.6	-7.96	6.08	-53.2	-7.44	6.27
5.1 - 5.2	-58.1	-8.46	9.58	-57.7	-7.92	5.58	-53.6	-7.42	5.74
5.2 - 5.3	-58.6	-8.40	8.60	-57.6	-7.84	5.10	-53.2	-7.47	6.48
5.3 - 5.4	-58.9	-8.50	9.10	-53.8	-7.60	7.01	-53.2	-7.45	6.38
5.4 - 5.5	-58.5	-8.44	9.02	-53.9	-7.60	6.90	-53.3	-7.49	6.66
5.5 - 5.6	-58.8	-8.40	8.40	-53.0	-7.43	6.45	-52.5	-7.27	5.67
5.6 - 5.7	-58.2	-8.38	8.84	-53.3	-7.42	6.07	-52.9	-7.31	5.57
5.7 - 5.8	-58.1	-8.37	8.86	-52.8	-7.37	6.15	-52.8	-7.28	5.43
5.8 - 5.9	-58.1	-8.36	8.78	-52.2	-7.25	5.77	-53.0	-7.26	5.09
5.9 - 6.0	-58.1	-8.36	8.78	-51.5	-7.21	6.11	-52.9	-7.18	4.52
6.0 - 6.1	-57.4	-8.28	8.84	-49.8	-6.97	5.99	-52.3	-7.13	4.71
6.1 - 6.2	-57.4	-8.23	8.44	-50.0	-6.99	5.96	-52.6	-7.16	4.66
6.2 - 6.3	-57.0	-8.19	8.52	-49.3	-6.86	5.65	-52.7	-7.15	4.46
6.3 - 6.4	-56.1	-8.03	8.14	-49.2	-6.88	5.86	-53.3	-7.21	4.33
6.4 - 6.5	-57.0	-8.11	7.88	-48.9	-6.84	5.85	-53.2	-7.21	4.47
6.5 - 6.6	-57.0	-8.18	8.44	-49.2	-6.89	5.96	-52.8	-7.23	5.03
6.6 - 6.7	-55.8	-8.00	8.20	-48.2	-6.68	5.27	-52.2	-7.11	4.71
6.7 - 6.8	-55.5	-7.94	8.02	-48.6	-6.82	5.97	-48.6	-6.84	6.05
6.8 - 6.9	-55.5	-7.89	7.62	-47.4	-6.64	5.75	-45.8	-6.44	5.80
6.9 - 7.0	-54.0	-7.75	8.00	-47.4	-6.62	5.64	-43.5	-6.17	5.82

ARTICLE IN PRESS

Geologia Croatica

Continuation

	S1 core			S2 core			C3 core		
depth (cm)	δD (‰)	$\delta^{18}O$ (‰)	d-excess (‰)	δD (‰)	$\delta^{18}O$ (‰)	d-excess (‰)	δD (‰)	$\delta^{18}O$ (‰)	d-excess (‰)
7.0 - 7.1	-50.7	-7.62	10.26	-44.5	-6.47	7.30	-43.6	-6.07	4.99
7.1 - 7.2	-50.3	-7.58	10.34	-44.1	-6.56	8.36	-43.5	-6.09	5.21
7.2 - 7.3	-49.8	-7.6	11.00	-43.4	-6.44	8.03	-43.7	-5.97	4.06
7.3 - 7.4	-49.6	-7.49	10.32	-44.0	-6.50	7.98	-43.9	-6.31	6.59
7.4 - 7.5	-48.5	-7.43	10.94	-43.8	-6.44	7.77	-45.2	-6.25	4.78
7.5 - 7.6	-48.3	-7.35	10.50	-44.2	-6.51	7.94	-44.0	-6.31	6.48
7.6 - 7.7	-46.9	-7.27	11.26	-44.9	-6.59	7.83	-44.1	-6.35	6.69
7.7 - 7.8	-46.6	-7.21	11.08	-44.5	-6.49	7.47	-43.3	-6.20	6.30
7.8 - 7.9	-45	-6.98	10.84	-43.6	-6.40	7.55	-43.8	-6.33	6.90
7.9 - 8.0	-45.2	-7	10.80	-42.7	-6.13	6.29	-42.8	-6.12	6.21
8.0 - 8.1	-44.6	-6.86	10.28	-44.8	-6.52	7.39	-44.7	-6.45	6.90
8.1 - 8.2	-42.7	-6.81	11.78	-44.8	-6.48	7.09	-43.4	-6.24	6.47
8.2 - 8.3	-42.3	-6.71	11.38	-45.5	-6.66	7.73	-44.0	-6.33	6.64
8.3 - 8.4	-42	-6.64	11.12	-45.1	-6.67	8.25	-43.9	-6.36	6.95
8.4 - 8.5	-40.9	-6.59	11.82	-44.5	-6.53	7.72	-43.4	-6.26	6.64
8.5 - 8.6	-40.4	-6.48	11.44	-45.4	-6.59	7.39	-43.0	-6.40	8.24
8.6 - 8.7	-40.1	-6.45	11.50	-45.1	-6.54	7.26	-42.6	-6.43	8.86
8.7 - 8.8	-39.9	-5.26	2.18	-43.8	-6.17	5.58	-42.1	-6.45	9.50
8.8 - 8.9	-38.5	-6.31	11.98	-43.1	-6.10	5.69	-42.5	-6.36	8.40
8.9 - 9.0	-37.7	-6.24	12.22	-43.0	-6.23	6.86	-42.4	-6.33	8.21
9.0 - 9.1	-37.9	-6.18	11.54	-43.5	-6.27	6.67	-44.6	-6.61	8.28
9.1 - 9.2	-37.7	-6.21	11.98	-44.1	-6.45	7.51	-44.1	-6.49	7.82
9.2 - 9.3	-37.3	-6.08	11.34	-44.0	-6.41	7.29	-43.1	-6.46	8.54
9.3 - 9.4	-37.3	-6.14	11.82	-44.2	-6.42	7.12	-41.9	-6.20	7.72
9.4 - 9.5	-37.7	-6.08	10.94	-43.6	-6.30	6.76	-41.3	-6.17	8.08
9.5 - 9.6	-37.5	-6.02	10.66	-43.7	-6.40	7.54	-40.5	-6.14	8.63
9.6 - 9.7	-37.4	-6.01	10.68	-42.3	-6.05	6.08	-41.0	-6.16	8.34
9.7 - 9.8	-37	-5.94	10.52	-42.7	-6.09	6.07	-39.9	-6.04	8.44
9.8 - 9.9	-37.7	-6.04	10.62	n.d.	n.d.	n.d.	-40.7	-6.02	7.47
9.9 - 10.0	-35.9	-5.67	9.46	-39.1	-5.32	3.53	-42.9	-6.41	8.33
10.0 - 10.1	-34.4	-5.21	7.28	-43.9	-6.28	6.38	-47.1	-6.81	7.41
10.1 - 10.2	-36.8	-5.68	8.64	-43.0	-6.36	7.86			
10.2 - 10.3	-37.4	-5.84	9.32	-43.1	-6.34	7.64			
10.3 - 10.4	-37.4	-5.79	8.92	-43.4	-6.44	8.06			
10.4 - 10.5	-37.9	-5.14	3.22	-42.6	-6.41	8.68			
10.5 - 10.6	-37.6	-6.08	11.04	-43.5	-6.34	7.24			
10.6 - 10.7	-38.2	-6.76	15.88	-43.0	-6.46	8.68			
10.7 - 10.8	-39	-6.82	15.56	-43.0	-6.32	7.59			
10.8 - 1.09	-39.1	-6.8	15.30	-41.5	-6.13	7.59			
10.9 - 11.0	-37.8	-6.49	14.12	-41.7	-6.09	7.02			
11.0 - 11.1	-39.5	-6.7	14.10	-42.7	-6.30	7.71			
11.1 - 11.2	-40.3	-6.82	14.26	-42.9	-6.37	8.00			
11.2 - 11.3	-40.6	-6.64	12.52	-43.5	-6.40	7.76			
11.3 - 11.4	-41.3	-6.68	12.14	-43.3	-6.36	7.60			
11.4 - 11.5	-42.2	-6.76	11.88	-43.1	-6.32	7.53			
11.5 - 11.6	-42.5	-6.73	11.34	-43.1	-6.30	7.36			
11.6 - 11.7	-42.1	-6.65	11.10	-42.7	-6.17	6.73			
11.7 - 11.8	-42.6	-6.64	10.52	-43.0	-6.18	6.45			
11.8 - 11.9	-43.3	-6.67	10.06	-42.8	-6.11	6.01			
11.9 - 12.0	-42.9	-6.48	8.94	-43.3	-6.15	5.95			
12.0 - 12.1	-44	-6.63	9.04	-44.4	-6.51	7.63			
12.1 - 12.2	-44.2	-6.6	8.60	-44.1	-6.47	7.70			
12.2 - 12.3	-44.2	-6.86	10.68	-44.6	-6.53	7.64			
12.3 - 12.4	-45	-6.93	10.44	-44.7	-6.59	8.07			
12.4 - 12.5	-43.5	-6.36	7.38	-44.2	-6.54	8.13			
12.5 - 12.6	-43.4	-6.38	7.64	-42.9	-6.53	9.29			
12.6 - 12.7	-45.0	-6.46	6.68	-43.5	-6.42	7.90			
12.7 - 12.8	-44.9	-6.53	7.34	-43.9	-6.48	7.97			
12.8 - 12.9	-45.7	-6.75	8.30	-43.7	-6.41	7.60			
12. 9 -13.0	-43.9	-6.49	8.02	-42.9	-6.22	6.84			
13.0 - 13.1	-45.7	-6.91	9.58	-43.2	-6.28	7.02			
13.1 - 13.2	-46.1	-7.00	9.90	-42.9	-6.34	7.79			
13.2 - 13.3	-46.1	-7.06	10.38	-42.1	-6.23	7.74			
13.3 - 13.4	-45.7	-7.08	10.94	-41.2	-6.14	7.98			
13.4 - 13.5	-46.2	-7.10	10.60	-41.1	-6.06	7.38			
13.5 - 13.6	-46.3	-7.08	10.34	-40.2	-5.86	6.71			
13.6 - 13.7	-46.4	-7.07	10.16	-40.7	-5.95	6.95			
13.7 - 13.8	-46.3	-6.92	9.06	-40.2	-5.91	7.12			
13.8 - 13.9	-45.1	-6.93	10.34	-39.3	-5.79	7.03			
13.9 - 14.0	-45.1	-6.97	10.66	-39.6	-5.84	7.10			
14.0 - 14.1	-44.9	-6.97	10.86						
14.1 - 14.2	-45.7	-7.08	10.94						
14.2 - 14.3	-45.8	-6.47	5.96						
14.3 - 14.4	-45.1	-6.37	5.86						
14.4 - 14.5	-44.9	-6.29	5.42						
14.5 - 14.6	-44.8	-6.45	6.80						
14.6 - 14.7	-44.6	-6.60	8.20						
14.7 - 14.8	-44.4	-6.64	8.72						
14.8 - 14.9	-44.4	-6.31	6.08						
14.9 - 15.0	-43.5	-6.11	5.38						

ARTICLE IN PRESS

Continuation

	C1			C2		
depth (m)	δD (‰)	$\delta^{18}O$ (‰)	d-excess (‰)	δD (‰)	$\delta^{18}O$ (‰)	d-excess (‰)
0.0 - 0.2	-25.4	-3.01	-1.28	-26.3	-4.64	10.84
0.2 - 0.4	-24.8	-3.85	6.00	-26.7	-4.87	12.32
0.4 - 0.6	-28.0	-4.65	9.19	-33.8	-5.32	8.68
0.6 - 0.8	-30.1	-4.67	7.31	-41.4	-6.11	7.45
0.8 - 1.0	-39.3	-5.23	2.59	-50.6	-6.93	4.81
1.0 - 1.2	-55.7	-7.09	0.98	-36.3	-5.60	8.56
1.2 - 1.4	-61.1	-7.82	1.50	-29.6	-4.01	2.51
1.4 - 1.6	-59.8	-7.68	1.68	-58.9	-8.08	5.72
1.6 - 1.8	-50.9	-6.52	1.25	-57.2	-8.00	6.79
1.8 - 2.0	-36.5	-5.13	4.48	-51.4	-7.35	7.39
2.0 - 2.2	-40.6	-5.45	2.99	-44.7	-6.41	6.60
2.2 - 2.4	-38.5	-5.14	2.61	-43.1	-6.27	7.08
2.4 - 2.6	-36.1	-4.80	2.31	-40.2	-5.93	7.23
2.6 - 2.8	-65.7	-5.04	4.64	-37.9	-5.68	7.49
2.8 - 3.0	-32.7	-4.57	3.86	-36.4	-5.49	7.51
3.0 - 3.2	-32.5	-4.92	6.92	-35.2	-5.36	7.62
3.2 - 3.4	-29.6	-4.34	5.14	-34.9	-5.28	7.33
3.4 - 3.6	-29.8	-4.37	5.17	-35.6	-5.29	6.70
3.6 - 3.8	-30.0	-4.16	3.24	-36.6	-5.39	6.45
3.8 - 4.0	-32.2	-4.39	2.94	-39.3	-5.66	5.98
4.0 - 4.2	-35.9	-5.00	4.11	-41.5	-6.04	6.79
4.2 -4.4	-39.3	-5.48	4.59	-42.7	-6.15	6.44
4.4 - 4.6	-42.1	-5.81	4.38	-44.1	-6.34	6.55
4.6 - 4.8	-43.1	-5.81	3.38	-45.7	-6.52	6.44
4.8 - 5.0	-48.7	-6.58	3.99	-47.1	-6.67	6.28
5.0 - 5.2	-50.9	-6.88	4.11	-48.3	-6.84	6.42
5.2 - 5.4	-48.2	-6.39	2.90	-48.0	-6.91	7.25
5.4 - 5.6	-48.9	-6.71	4.73	-47.8	-6.87	7.08
5.6 - 5.8	-46.9	-6.44	4.59	-46.8	-6.80	7.61
5.8 - 6.0	-44.6	-6.20	4.98	-44.9	-6.50	7.11
6.0 - 6.2	-38.3	-5.28	3.92	-43.2	-6.28	7.10
6.2 - 6.4	-43.6	-6.34	7.14	-41.9	-6.19	7.65
6.4 - 6.6	-42.2	-5.96	5.49	-41.0	-6.06	7.52
6.6 - 6.8	-41.3	-5.87	5.67	-39.9	-5.85	6.92
6.8 - 7.0	-39.9	-5.58	4.72	-38.7	-5.75	7.27
7.0 - 7.2	-38.8	-5.19	2.76	-39.6	-5.92	7.73
7.2 - 7.4	-38.0	-5.13	3.05	-39.0	-5.73	6.87
7.4 - 7.6	-38.4	-5.19	3.16	-38.8	-5.72	7.00
7.6 - 7.8	-37.8	-5.18	3.63	-38.0	-5.54	6.35
7.8 - 8.0	-36.0	-4.86	2.90	-36.9	-5.39	6.26
8.0 - 8.2	-36.6	-4.92	2.74	-37.7	-5.56	6.80
8.2 - 8.4	-34.9	-4.72	2.88	-37.5	-5.65	7.64
8.4 - 8.6	-35.3	-4.78	2.94	-37.1	-5.57	7.42
8.6 - 8.8	-34.6	-4.93	4.85	-37.0	-5.55	7.41
8.8 - 9.0	-33.7	-4.80	4.75	-36.7	-5.49	7.23
9.0 - 9.2	-30.9	-4.22	2.86	-36.2	-5.43	7.18
9.2 - 9.4	-30.2	-4.29	4.07	-36.3	-5.48	7.54
9.4 - 9.6	-30.5	-4.38	4.53	-36.0	-5.37	6.99
9.6 - 9.8	-30.3	-4.40	4.98	-35.8	-5.30	6.53
9.8 - 10.0	-29.2	-4.02	2.94	-34.9	-5.15	6.32

ARTICLE IN PRESS

Geologia Croatica

Continuation

	C1			C2		
depth(cm)	δD (‰)	$\delta^{18}O$ (‰)	d-excess (‰)	δD (‰)	$\delta^{18}O$ (‰)	d-excess (‰)
10.0 - 10.2	-27.5	-3.59	1.21	-35.1	-5.28	7.09
10.2 - 10.4	-24.7	-2.65	-3.51	-35.0	-5.30	7.45
10.4 - 10.6	-22.5	-2.20	-4.85	-35.0	-5.21	6.69
10.6 - 10.8	-23.9	-2.55	-3.55	-34.7	-5.19	6.84
10.8 - 11.0	-24.4	-2.69	-2.91	-34.0	-5.21	7.62
11.0 - 11.2	-28.0	-3.70	1.65	-35.2	-5.19	6.35
11.2 - 11.4	-27.5	-3.49	0.42	-34.2	-4.93	5.30
11.4 - 11.6	-26.3	-3.30	0.08	-33.6	-5.03	6.66
11.6 - 11.8	-29.1	-3.90	2.06	-32.9	-4.96	6.73
11.8 - 12.0	-26.1	-3.17	-0.75	-32.7	-4.69	4.80
12.0 - 12.2	-25.6	-3.14	-0.51	-33.0	-4.78	5.19
12.2 - 12.4	-27.1	-3.51	0.91	-32.5	-4.76	5.55
12.4 - 12.6	-25.8	-3.17	-0.44	-32.3	-4.70	5.32
12.6 - 12.8	-25.8	-3.12	-0.80	-32.5	-4.65	4.76
12.8 - 13.0	-26.3	-3.37	0.66	-30.4	-4.35	4.47
13.0 - 13.2	-24.0	-2.79	-1.60	-32.5	-4.55	3.93
13.2 - 13.4	-26.3	-3.49	1.61	-32.6	-4.65	4.58
13.4 - 13.6	-27.7	-3.84	2.99	-31.3	-4.56	5.15
13.6 - 13.8	-26.8	-3.63	2.28	-28.7	-3.72	1.06
13.8 - 14.0	-25.9	-3.38	1.13	-25.8	-3.24	0.04
14.0 - 14.2	-24.2	-2.89	-1.06	-27.0	-3.59	1.73
14.2 - 14.4	-24.8	-3.18	0.68	-23.7	-2.61	-2.79
14.4 - 14.6	-24.8	-3.13	0.22	-28.6	-3.89	2.51
14.6 - 14.8	-24.4	-3.06	0.11	-21.6	-2.13	-4.54
14.8 - 15.0	-20.5	-2.07	-3.97	-16.1	-1.16	-6.88
15.0 - 15.2	-22.7	-2.61	-1.79			
15.2 - 15.4	-25.7	-3.38	1.34			
15.4 - 15.6	-22.7	-2.52	-2.60			
15.6 - 15.8	-25.0	-3.18	0.41			
15.8 - 16.0	-20.9	-2.16	-3.56			
16.0 - 16.2	-24.1	-2.93	-0.63			
16.2 - 16.4	-24.4	-2.99	-0.42			
16.4 - 16.6	-24.5	-3.11	0.34			
16.6 - 16.8	-27.3	-3.67	2.03			
16.8 - 17.0	-26.3	-3.32	0.27			
17.0 - 17.2	-29.3	-3.99	2.62			
17.2 - 17.4	-29.2	-3.89	1.87			
18.4 - 17.6	-32.7	-4.47	3.02			
17.6 - 17.8	-34.5	-4.73	3.32			
17.8 - 18.0	-34.3	-4.46	1.41			
18.0 - 18.2	-31.0	-3.67	-1.71			
18.2 - 18.4	-34.6	-4.54	1.66			
18.4 - 18.6	-37.5	-5.01	2.54			
18.6 - 18.8	-38.2	-5.05	2.21			
18.8 - 19.0	-38.9	-5.12	2.04			
19.0 - 19.2	-40.2	-5.46	3.43			
19.2 - 19.4	-39.7	-5.36	3.18			
19.4 - 19.6	-39.5	-5.19	2.06			
19.6 - 19.8	-39.7	-5.15	1.44			
19.8 - 20.0	-35.4	-4.34	-0.61			

ARTICLE IN PRESS

Table A2. Soil water content (mm) and three phase distribution (%) of 0.1 m core samples.

S1 core depth (m)	water amount (mm)	Three phase distribution (%) Gas phase	Liquid phase	Solid phase
0.0 - 0.1	53	9.3	52	38.7
0.1- 0.2	54	11.1	53	35.9
0.2 - 0.3	51	14.9	50	35.1
0.3 - 0.4	55	16	54	30
0.4 - 0.5	60	15	59	26
0.5 - 0.6	57	18.1	56	25.9
0.6 - 0.7	65	13	64	23
0.7 - 0.8	64	9.9	63	27.1
0.8 - 0.9	59	15.5	58	26.5
0.9 - 1.0	61	13.5	60	26.5
1.0 - 1.1	65	8.7	64	27.3
1.1 - 1.2	61	21.8	60	18.2
1.2 - 1.3	64	9	63	28
1.3 - 1.4	61	11.8	60	28.2
1.4 - 1.5	59	17.8	58	24.2
1.5 -1.6	49	12.6	48	39.4
1.6 - 1.7	52	19.2	51	29.8
1.7 - 1.8	51	19.9	50	30.1
1.8 - 1.9	51	11	50	39
1.9 - 2.0	46	27.9	45	27.1
2.0 - 2.1	57	27.5	56	16.5
2.1 - 2.2	61	11.8	60	28.2
2.2 - 2.3	59	27	58	15
2.3 - 2.4	60	18.8	59	22.2
2.4 - 2.5	54	21.9	53	25.1
2.5 - 2.6	57	19.5	56	24.5
2.6 - 2.7	53	11.9	52	36.1
2.7 - 2.8	62	14.75	61	24.25
2.8 - 2.9	51	26.2	50	23.8
2.9 - 3.0	48	13.8	47	39.2
3.0 - 3.1	46	21	45	34
3.1 - 3.2	45	21.3	44	34.7
3.2 - 3.3	45	21.6	44	34.4
3.3 - 3.4	50	14.1	49	36.9
3.4 - 3.5	49	18.6	48	33.4
3.5 - 3.6	48	25.2	47	27.8
3.6 - 3.7	48	27.5	47	25.5
3.7 - 3.8	48	28.9	47	24.1
3.8 - 3.9	50	23.2	49	27.8
3.9 - 4.0	45	27.5	44	28.5
4.0 - 4.1	42	34.7	41	24.3
4.1 - 4.2	48	25.5	47	27.5
4.2 - 4.3	51	19.6	50	30.4
4.3 - 4.4	53	19.3	52	28.7
4.4 - 4.5	54	11.7	53	35.3
4.5 - 4.6	53	10.8	52	37.2
4.6 - 4.7	54	14.7	53	32.3
4.7 - 4.8	53	10.9	52	37.1
4.8 - 4.9	52	19.2	51	29.8
4.9 - 5.0	55	15.4	54	30.6
5.0 - 5.1	54	14.3	53	32.7
5.1 - 5.2	59	2	58	40
5.2 - 5.3	60	4.8	59	36.2
5.3 - 5.4	60	9.8	59	31.2
5.4 - 5.5	59	17.8	58	24.2
5.5 - 5.6	57	14.9	56	29.1
5.6 - 5.7	57	15.4	56	28.6
5.7 - 5.8	54	11.2	53	35.8
5.8 - 5.9	55	12.9	54	33.1
5.9 - 6.0	53	13.2	52	34.8
6.0 - 6.1	58	0.7	57	42.3
6.1 - 6.2	60	3.1	59	37.9
6.2 - 6.3	64	7.7	63	29.3
6.3 - 6.4	62	7.9	61	31.1
6.4 - 6.5	59	7.3	58	34.7
6.5 - 6.6	64	0.8	63	36.2
6.6 - 6.7	61	6.3	60	33.7
6.7 - 6.8	63	7.1	62	30.9
6.8 - 6.9	62	6.9	61	32.1
6.9 - 7.0	60	4.5	59	36.5

S1 core depth (m)	water amount (mm)	Three phase distribution (%) Gas phase	Liquid phase	Solid phase
7.0 - 7.1	58	2.5	57	40.5
7.1 - 7.2	58	4.6	57	38.4
7.2 - 7.3	58	6.9	57	36.1
7.3 - 7.4	50	3.7	49	47.3
7.4 - 7.5	53	2.2	52	45.8
7.5 - 7.6	56	1.4	55	43.6
7.6 - 7.7	55	9.9	54	36.1
7.7 - 7.8	55	1.6	54	44.4
7.8 - 7.9	47	8.9	46	45.1
7.9 - 8.0	52	17.6	51	31.4
8.0 - 8.1	59	6	58	36
8.1 - 8.2	55	9.9	54	36.1
8.2 - 8.3	60	7.9	59	33.1
8.3 - 8.4	50	6	49	45
8.4 - 8.5	55	4.4	54	41.6
8.5 - 8.6	43	7.2	42	50.8
8.6 - 8.7	56	7.4	55	37.6
8.7 - 8.8	59	3.4	58	38.6
8.8 - 8.9	55	11	54	35
8.9 - 9.0	57	3.5	56	40.5
9.0 - 9.1	51	17.9	50	32.1
9.1 - 9.2	45	20	44	36
9.2 - 9.3	41	28.8	44	27.2
9.3 - 9.4	38	36.5	37	26.5
9.4 - 9.5	34	35.3	34	30.7
9.5 - 9.6	30	44.7	29	26.3
9.6 - 9.7	32	20.7	35	44.3
9.7 - 9.8	34	32.1	33	34.9
9.8 - 9.9	33	20.9	38	41.1
9.9 - 10.0	32	45.1	31	23.9
10.0 - 10.1	33	n.d.	n.d.	n.d.
10.1 - 10.2	32	n.d.	n.d.	n.d.
10.2 - 10.3	32	47.5	32	20.5
10.3 - 10.4	34	36.6	33	30.4
10.4 - 10.5	31	46.9	29	24.1
10.5 - 10.6	29	46.5	28	25.5
10.6 - 10.7	28	34.7	30	35.3
10.7 - 10.8	28	30.8	27	42.2
10.8 - 1.09	27	33.8	28	38.2
10.9 - 11.0	25	30.8	25	44.2
11.0 - 11.1	28	39.9	28	32.1
11.1 - 11.2	30	37.3	29	33.7
11.2 - 11.3	29	36.5	28	35.5
11.3 - 11.4	28	33.7	27	39.3
11.4 - 11.5	28	36.1	29	34.9
11.5 - 11.6	28	40	27	33
11.6 - 11.7	30	40	27	33
11.7 - 11.8	33	22	32	46
11.8 - 11.9	29	40.1	25	34.9
11.9 - 12.0	25	39.4	25	35.6
12.0 - 12.1	26	46.3	24	29.7
12.1 - 12.2	28	35.7	27	37.3
12.2 - 12.3	28	48	26	26
12.3 - 12.4	28	40	27	33
12.4 - 12.5	28	46.8	25	28.2
12.5 - 12.6	28	30.6	27	42.4
12.6 - 12.7	28	32.5	27	40.5
12.7 - 12.8	28	31.4	27	41.6
12.8 - 12.9	26	44.4	23	32.6
12. 9 -13.0	24	42.2	24	33.8
13.0 - 13.1	25	40	27	33
13.1 - 13.2	26	30.7	26	43.3
13.2 - 13.3	29	30.5	27	42.5
13.3 - 13.4	31	32	30	38
13.4 - 13.5	31	32.7	27	40.3
13.5 - 13.6	32	38	31	31
13.6 - 13.7	32	31.9	29	39.1
13.7 - 13.8	33	38.8	32	29.2
13.8 - 13.9	32	30.4	28	41.6
13.9 - 14.0	31	32.2	30	37.8
14.0 - 14.1	30	37.4	27	35.6
14.1 - 14.2	30	39.4	29	31.6
14.2 - 14.3	30	39.5	29	31.5
14.3 - 14.4	30	34	29	37
14.4 - 14.5	30	37.8	31	31.2
14.5 - 14.6	30	20.8	29	50.2
14.6 - 14.7	31	38.4	29	32.6
14.7 - 14.8	32	37	31	32
14.8 - 14.9	31	38.9	31	30.1
14.9 - 15.0	31	37.2	30	32.8

ARTICLE IN PRESS

Geologia Croatica

Continuation

C3 core depth (m)	water amount (mm)	Three phase distribution (%)		
		Gas phase	Liquid phase	Solid phase
0.0 - 0.1	32	35.8	31	33.2
0.1- 0.2	39	29	38	33
0.2 - 0.3	47	12.5	46	41.5
0.3 - 0.4	46	12	45	43
0.4 - 0.5	52	26.4	51	22.6
0.5 - 0.6	60	13.7	59	27.3
0.6 - 0.7	61	17.4	60	22.6
0.7 - 0.8	67	16.5	66	17.5
0.8 - 0.9	69	12.9	68	19.1
0.9 - 1.0	63	26	62	12
1.0 - 1.1	68	13.1	67	19.9
1.1 - 1.2	58	10.5	57	32.5
1.2 - 1.3	71	18.5	70	11.5
1.3 - 1.4	72	2.1	71	26.9
1.4 - 1.5	69	17.1	68	14.9
1.5 -1.6	71	18	70	12
1.6 - 1.7	68	16	67	17
1.7 - 1.8	64	28.6	63	8.4
1.8 - 1.9	67	12.9	66	21.1
1.9 - 2.0	75	5	74	21
2.0 - 2.1	77	6	76	18
2.1 - 2.2	77	5.4	76	18.6
2.2 - 2.3	76	4.8	75	20.2
2.3 - 2.4	76	5.5	75	19.5
2.4 - 2.5	76	6.6	75	18.4
2.5 - 2.6	68	17.7	67	15.3
2.6 - 2.7	72	2.3	71	26.7
2.7 - 2.8	71	10	70	20
2.8 - 2.9	74	11	73	16
2.9 - 3.0	70	14.7	69	16.3
3.0 - 3.1	67	5	66	29
3.1 - 3.2	66	2.6	65	32.4
3.2 - 3.3	69	18.4	68	13.6
3.3 - 3.4	67	13.4	66	20.6
3.4 - 3.5	69	6.9	68	25.1
3.5 - 3.6	68	17.8	67	15.2
3.6 - 3.7	60	7.9	59	33.1
3.7 - 3.8	67	2.8	66	31.2
3.8 - 3.9	69	6.1	68	25.9
3.9 - 4.0	59	17.4	58	24.6
4.0 - 4.1	67	5	66	29
4.1 - 4.2	68	2.8	67	30.2
4.2 - 4.3	65	2.2	64	33.8
4.3 - 4.4	55	8.2	54	37.8
4.4 - 4.5	69	3.8	68	28.2
4.5 - 4.6	59	4.9	58	37.1
4.6 - 4.7	49	6	48	46
4.7 - 4.8	48	14.3	47	38.7
4.8 - 4.9	47	22.6	46	31.4
4.9 - 5.0	49	24.4	48	27.6

C3 core depth (m)	water amount (mm)	Three phase distribution (%)		
		Gas phase	Liquid phase	Solid phase
5.0 - 5.1	65	11.6	64	24.4
5.1 - 5.2	66	10.2	65	24.8
5.2 - 5.3	66	8.4	65	26.6
5.3 - 5.4	72	4.5	71	24.5
5.4 - 5.5	69	9.9	68	22.1
5.5 - 5.6	68	10.5	67	22.5
5.6 - 5.7	66	11.7	65	23.3
5.7 - 5.8	68	11.5	67	21.5
5.8 - 5.9	69	9.7	68	22.3
5.9 - 6.0	67	8.8	66	25.2
6.0 - 6.1	65	7.5	64	28.5
6.1 - 6.2	67	4.8	66	29.2
6.2 - 6.3	63	11.5	62	26.5
6.3 - 6.4	62	6.2	61	32.8
6.4 - 6.5	87	10.5	55	34.5
6.5 - 6.6	62	4.4	61	34.6
6.6 - 6.7	61	3	60	37
6.7 - 6.8	60	4	59	37
6.8 - 6.9	57	4.8	56	39.2
6.9 - 7.0	57	7.2	56	36.8
7.0 - 7.1	61	0.2	60	39.8
7.1 - 7.2	53	1.2	52	46.8
7.2 - 7.3	56	6.2	55	38.8
7.3 - 7.4	55	3.8	54	42.2
7.4 - 7.5	55	6.1	54	39.9
7.5 - 7.6	53	7.2	52	40.8
7.6 - 7.7	53	14.8	52	33.2
7.7 - 7.8	51	6.4	50	43.6
7.8 - 7.9	52	3.4	51	45.6
7.9 - 8.0	53	1.2	52	46.8
8.0 - 8.1	55	0.6	54	45.4
8.1 - 8.2	54	1.9	53	45.1
8.2 - 8.3	51	4.8	50	45.2
8.3 - 8.4	53	2.8	52	45.2
8.4 - 8.5	53	4	52	44
8.5 - 8.6	52	3.6	51	45.4
8.6 - 8.7	48	5.5	47	47.5
8.7 - 8.8	52	3.7	51	45.3
8.8 - 8.9	51	3.1	50	46.9
8.9 - 9.0	50	3	49	48
9.0 - 9.1	53	0.3	52	47.7
9.1 - 9.2	52	1.1	51	47.9
9.2 - 9.3	52	2.3	51	46.7
9.3 - 9.4	52	2.4	51	46.6
9.4 - 9.5	50	5.7	49	45.3
9.5 - 9.6	151	7	48	45
9.6 - 9.7	48	7.4	47	45.6
9.7 - 9.8	49	5.9	48	46.1
9.8 - 9.9	53	1.3	52	46.7
9.9 - 10.0	52	4.6	51	44.4
10.0 - 10.1	53	2.4	52	45.6

ARTICLE IN PRESS

Continuation

C1 core depth (m)	water amount (mm)	Three phase distribution (%)		
		Gas phase	Liquid phase	Solid phase
0.0 - 0.2	144	25	47	28
0.2 - 0.4	98	25.4	48	26.6
0.4 - 0.6	96	30.6	47	22.4
0.6 - 0.8	94	24.8	46	29.2
0.8 - 1.0	92	26	55	19
1.0 - 1.2	100	n.d.	n.d.	n.d.
1.2 - 1.4	98	n.d.	n.d.	n.d.
1.4 - 1.6	100	n.d.	n.d.	n.d.
1.6 - 1.8	112	n.d.	n.d.	n.d.
1.8 - 2.0	108	n.d.	n.d.	n.d.
2.0 - 2.2	100	n.d.	n.d.	n.d.
2.2 - 2.4	90	n.d.	n.d.	n.d.
2.4 - 2.6	77	n.d.	n.d.	n.d.
2.6 - 2.8	73	n.d.	n.d.	n.d.
2.8 - 3.0	79	n.d.	n.d.	n.d.
3.0 - 3.2	82	n.d.	n.d.	n.d.
3.2 - 3.4	84	n.d.	n.d.	n.d.
3.4 - 3.6	73	n.d.	n.d.	n.d.
3.6 - 3.8	82	n.d.	n.d.	n.d.
3.8 - 4.0	73	n.d.	n.d.	n.d.
4.0 - 4.2	96	n.d.	n.d.	n.d.
4.2 -4.4	63	n.d.	n.d.	n.d.
4.4 - 4.6	128	n.d.	n.d.	n.d.
4.6 - 4.8	100	n.d.	n.d.	n.d.
4.8 - 5.0	104	16.5	55	28.5
5.0 - 5.2	110	17.8	52.5	29.7
5.2 - 5.4	102	n.d.	n.d.	n.d.
5.4 - 5.6	106	n.d.	n.d.	n.d.
5.6 - 5.8	112	n.d.	n.d.	n.d.
5.8 - 6.0	96	n.d.	n.d.	n.d.
6.0 - 6.2	104	n.d.	n.d.	n.d.
6.2 - 6.4	106	n.d.	n.d.	n.d.
6.4 - 6.6	108	n.d.	n.d.	n.d.
6.6 - 6.8	110	n.d.	n.d.	n.d.
6.8 - 7.0	106	n.d.	n.d.	n.d.
7.0 - 7.2	102	n.d.	n.d.	n.d.
7.2 - 7.4	110	n.d.	n.d.	n.d.
7.4 - 7.6	135	n.d.	n.d.	n.d.
7.6 - 7.8	118	n.d.	n.d.	n.d.
7.8 - 8.0	110	n.d.	n.d.	n.d.
8.0 - 8.2	122	n.d.	n.d.	n.d.
8.2 - 8.4	112	n.d.	n.d.	n.d.
8.4 - 8.6	108	n.d.	n.d.	n.d.
8.6 - 8.8	112	n.d.	n.d.	n.d.
8.8 - 9.0	108	n.d.	n.d.	n.d.
9.0 - 9.2	106	n.d.	n.d.	n.d.
9.2 - 9.4	90	n.d.	n.d.	n.d.
9.4 - 9.6	104	n.d.	n.d.	n.d.
9.6 - 9.8	100	n.d.	n.d.	n.d.
9.8 - 10.0	52	18.3	47	34.7

C2 core depth (m)	water amount (mm)	Three phase distribution (%)		
		Gas phase	Liquid phase	Solid phase
0.0 - 0.2	77	23	38	39
0.2 - 0.4	116	28.9	57	14.1
0.4 - 0.6	120	12.5	59	28.5
0.6 - 0.8	108	30	53	17
0.8 - 1.0	118	27.3	58	14.7
1.0 - 1.2	119	n.d.	n.d.	n.d.
1.2 - 1.4	126	n.d.	n.d.	n.d.
1.4 - 1.6	130	11	64	25
1.6 - 1.8	130	17.5	64	18.5
1.8 - 2.0	132	16.5	65	18.5
2.0 - 2.2	141	n.d.	69	n.d.
2.2 - 2.4	149	4.7	73	22.3
2.4 - 2.6	145	4.4	71	24.6
2.6 - 2.8	143	2.2	70	27.8
2.8 - 3.0	143	3.5	70	26.5
3.0 - 3.2	139	11.4	68	20.6
3.2 - 3.4	132	16.7	65	18.3
3.4 - 3.6	139	9	68	23
3.6 - 3.8	141	19.5	69	11.5
3.8 - 4.0	135	18.5	66	15.5
4.0 - 4.2	130	3.5	64	32.5
4.2 -4.4	124	17.5	61	21.5
4.4 - 4.6	102	21.4	50	28.6
4.6 - 4.8	120	11.8	59	29.2
4.8 - 5.0	115	n.d.	56.5	n.d.
5.0 - 5.2	110	16.9	54	29.1
5.2 - 5.4	102	12	50	38
5.4 - 5.6	102	11.5	50	38.5
5.6 - 5.8	108	9.7	53	37.3
5.8 - 6.0	105	n.d.	51.5	n.d.
6.0 - 6.2	102	19.3	50	30.7
6.2 - 6.4	108	2.9	53	44.1
6.4 - 6.6	110	19	54	27
6.6 - 6.8	104	13	51	36
6.8 - 7.0	105	n.d.	51.5	n.d.
7.0 - 7.2	106	12	52	36
7.2 - 7.4	102	28	50	22
7.4 - 7.6	104	28.7	51	20.3
7.6 - 7.8	92	22.9	45	32.1
7.8 - 8.0	94	n.d.	46	n.d.
8.0 - 8.2	96	24	47	29
8.2 - 8.4	92	23	45	32
8.4 - 8.6	98	26.6	48	25.4
8.6 - 8.8	100	29.1	49	21.9
8.8 - 9.0	100	12.4	49	38.6
9.0 - 9.2	104	18.3	51	30.7
9.2 - 9.4	104	16	51	33
9.4 - 9.6	104	16.5	51	32.5
9.6 - 9.8	100	13.7	49	37.3
9.8 - 10.0	104	16.6	51	32.4
10.0 - 10.2	102	15.6	50	34.4
10.2 - 10.4	102	16.6	50	33.4
10.4 - 10.6	102	16.3	50	33.7
10.6 - 10.8	104	15.5	51	33.5
10.8 - 11.0	106	1.5	52	46.5
11.0 - 11.2	100	19.3	49	31.7
11.2 - 11.4	96	17	47	36
11.4 - 11.6	98	16.4	48	35.6
11.6 - 11.8	90	11	44	45
11.8 - 12.0	78	n.d.	38.5	n.d.
12.0 - 12.2	67	37.2	33	29.8
12.2 - 12.4	55	30.7	27	42.3
12.4 - 12.6	55	31.6	27	41.4
12.6 - 12.8	49	30.1	24	45.9
12.8 - 13.0	49	n.d.	n.d.	n.d.
13.0 - 13.2	49	31.5	24	44.5
13.2 - 13.4	45	30.1	22	47.9
13.4 - 13.6	47	30.5	23	46.5
13.6 - 13.8	49	31	24	45
13.8 - 14.0	46	n.d.	n.d.	n.d.
14.0 - 14.2	47	n.d.	n.d.	n.d.
14.2 - 14.4	43	40	21	39
14.4 - 14.6	49	34.2	24	41.8
14.6 - 14.8	46	n.d.	n.d.	n.d.
14.8 - 15.0	48	n.d.	n.d.	n.d.

ARTICLE IN PRESS

Geologia Croatica

Continuation

S2 core depth (m)	water amount (mm)	Three phase distribution (%)		
		Gas phase	Liquid phase	Solid phase
0.0 - 0.1	51	13.9	50	36.1
0.1- 0.2	47	9.4	46	44.6
0.2 - 0.3	47	27.9	46	26.1
0.3 - 0.4	50	19.8	49	31.2
0.4 - 0.5	50	22.6	49	28.4
0.5 - 0.6	50	36.9	49	14.1
0.6 - 0.7	47	21.3	46	32.7
0.7 - 0.8	53	25.2	52	22.8
0.8 - 0.9	53	28.9	52	19.1
0.9 - 1.0	54	29.2	53	17.8
1.0 - 1.1	50	34.4	49	16.6
1.1 - 1.2	58	14	57	29
1.2 - 1.3	45	35.5	44	20.5
1.3 - 1.4	54	8.8	53	38.2
1.4 - 1.5	58	17.7	57	25.3
1.5 -1.6	54	10.9	53	36.1
1.6 - 1.7	63	10.7	62	27.3
1.7 - 1.8	61	9.8	60	30.2
1.8 - 1.9	54	19.8	53	27.2
1.9 - 2.0	55	10.5	54	35.5
2.0 - 2.1	59	17.2	58	24.8
2.1 - 2.2	59	16	58	26
2.2 - 2.3	66	17.5	65	17.5
2.3 - 2.4	66	8.9	65	26.1
2.4 - 2.5	64	18	63	19
2.5 - 2.6	57	18.7	56	25.3
2.6 - 2.7	59	1.2	58	40.8
2.7 - 2.8	62	5	61	34
2.8 - 2.9	55	5.4	54	40.6
2.9 - 3.0	57	1.3	56	42.7
3.0 - 3.1	54	8.5	53	38.5
3.1 - 3.2	54	8.7	53	38.3
3.2 - 3.3	53	9.4	52	38.6
3.3 - 3.4	51	9	50	41
3.4 - 3.5	47	2.8	46	51.2
3.5 - 3.6	54	4.5	53	42.5
3.6 - 3.7	52	16	51	33
3.7 - 3.8	53	8.8	52	39.2
3.8 - 3.9	55	3	54	43
3.9 - 4.0	59	8.2	58	33.8
4.0 - 4.1	52	4.3	51	44.7
4.1 - 4.2	58	4.5	57	38.5
4.2 - 4.3	55	15	54	31
4.3 - 4.4	54	1.8	53	45.2
4.4 - 4.5	56	1.6	55	43.4
4.5 - 4.6	57	4.6	56	39.4
4.6 - 4.7	53	1.2	52	46.8
4.7 - 4.8	48	19.5	47	33.5
4.8 - 4.9	51	18.3	50	31.7
4.9 - 5.0	54	16.8	53	30.2
5.0 - 5.1	58	1.1	57	41.9
5.1 - 5.2	62	5.9	61	33.1
5.2 - 5.3	60	3.8	59	37.2
5.3 - 5.4	60	2.1	59	38.9
5.4 - 5.5	59	2.4	58	39.6
5.5 - 5.6	47	26.1	46	27.9
5.6 - 5.7	53	18.9	52	29.1
5.7 - 5.8	57	4.5	56	39.5
5.8 - 5.9	56	1.2	55	43.8
5.9 - 6.0	56	4.7	55	40.3
6.0 - 6.1	53	7	52	41
6.1 - 6.2	52	8.2	51	40.8
6.2 - 6.3	50	5.6	49	45.4
6.3 - 6.4	51	7	50	43
6.4 - 6.5	46	8.6	45	46.4
6.5 - 6.6	55	9.2	54	36.8
6.6 - 6.7	50	8.6	49	42.4
6.7 - 6.8	53	8.9	52	39.1
6.8 - 6.9	48	7	47	46
6.9 - 7.0	51	1.9	50	48.1

S2 core depth (m)	water amount (mm)	Three phase distribution (%)		
		Gas phase	Liquid phase	Solid phase
7.0 - 7.1	45	6.7	44	49.3
7.1 - 7.2	44	2.5	43	54.5
7.2 - 7.3	41	9.9	40	50.1
7.3 - 7.4	42	18.2	41	40.8
7.4 - 7.5	46	6.3	45	48.7
7.5 - 7.6	47	10	46	44
7.6 - 7.7	42	18.2	41	40.8
7.7 - 7.8	43	1.3	42	56.7
7.8 - 7.9	41	11.9	40	48.1
7.9 - 8.0	41	15.9	40	44.1
8.0 - 8.1	44	18.6	43	38.4
8.1 - 8.2	49	4.7	48	47.3
8.2 - 8.3	37	9.9	36	54.1
8.3 - 8.4	46	16	45	39
8.4 - 8.5	37	21.7	36	42.3
8.5 - 8.6	38	11.3	37	51.7
8.6 - 8.7	36	38.7	35	26.3
8.7 - 8.8	36	20.8	35	44.2
8.8 - 8.9	35	38.8	34	27.2
8.9 - 9.0	35	21.9	34	44.1
9.0 - 9.1	34	38.8	33	28.2
9.1 - 9.2	36	38	35	27
9.2 - 9.3	39	23.6	38	38.4
9.3 - 9.4	38	22.9	37	40.1
9.4 - 9.5	37	39	36	25
9.5 - 9.6	36	39	35	26
9.6 - 9.7	38	24.1	37	38.9
9.7 - 9.8	38	24.5	37	38.5
9.8 - 9.9	37	22.9	36	41.1
9.9 - 10.0	35	24.6	34	41.4
10.0 - 10.1	45	14.9	44	41.1
10.1 - 10.2	40	18.4	39	42.6
10.2 - 10.3	47	15	46	39
10.3 - 10.4	45	12.6	44	43.4
10.4 - 10.5	47	16.5	46	37.5
10.5 - 10.6	39	5.4	38	56.6
10.6 - 10.7	50	3	49	48
10.7 - 10.8	50	1.8	49	49.2
10.8 - 1.09	45	13.3	44	42.7
10.9 - 11.0	49	18.1	48	33.9
11.0 - 11.1	49	18.1	48	33.9
11.1 - 11.2	50	10.2	49	40.8
11.2 - 11.3	50	2.6	49	48.4
11.3 - 11.4	49	1.3	48	50.7
11.4 - 11.5	50	5.1	49	45.9
11.5 - 11.6	52	3.8	51	45.2
11.6 - 11.7	51	9.3	50	40.7
11.7 - 11.8	45	16.2	44	39.8
11.8 - 11.9	47	6	46	48
11.9 - 12.0	51	4.3	50	45.7
12.0 - 12.1	53	2	52	46
12.1 - 12.2	57	3.3	56	40.7
12.2 - 12.3	53	17	52	31
12.3 - 12.4	56	2	55	43
12.4 - 12.5	59	6.4	58	35.6
12.5 - 12.6	55	3.6	54	42.4
12.6 - 12.7	52	10	51	39
12.7 - 12.8	54	4	53	43
12.8 - 12.9	56	4.9	55	40.1
12. 9 -13.0	51	16	50	34
13.0 - 13.1	60	6.2	59	34.8
13.1 - 13.2	57	7	56	37
13.2 - 13.3	54	8.3	53	38.7
13.3 - 13.4	60	4.5	59	36.5
13.4 - 13.5	62	6.4	61	32.6
13.5 - 13.6	54	8.2	53	38.8
13.6 - 13.7	58	5.9	57	37.1
13.7 - 13.8	57	5.3	56	38.7
13.8 - 13.9	56	10	55	35
13.9 - 14.0	56	10.4	55	34.6

ARTICLE IN PRESS

Table A3. Precipitation data using DFM calculation for all cores.

month	average temperature (℃)	precipitation total amount(mm)	δD (‰)	$\delta^{18}O$ (‰)	d-excess (‰)
Jan-2005	5	48	-50	-9.5	26
Feb-2005	6	100	-44	-7.6	16.8
Mar-2005	9	128	-24	-5.1	16.8
Apr-2005	17	92	-14	-3.2	11.6
May-2005	21	135	-26	-4.6	10.8
Jun-2005	26	93	-38	-5.9	9.2
Jul-2005	28	365	-48	-7.4	11.2
Aug-2005	28	73	-66	-9.7	11.6
Sep-2005	27	147	-89	-11.7	4.6
Oct-2005	21	41	-20	-4.4	15.2
Nov-2005	14	73	-18	-4.9	21.2
Dec-2005	5	31	-16	-6.3	34.4
Jan-2006	6	61	-40	-6.6	12.8
Feb-2006	8	118	-28	-5.8	18.4
Mar-2006	10	102	-20	-4.9	19.2
Apr-2006	15	216	-14	-3.3	12.4
May-2006	21	214	-21	-4.3	13.4
Jun-2006	24	642	-51	-7.8	11.4
Jul-2006	28	789	-39	-6.1	9.8
Aug-2006	29	428	-62	-8.6	6.8
Sep-2006	25	94	-33	-5.9	14.2
Oct-2006	21	11	-7	-2.6	13.8
Nov-2006	15	81	-56	-8.9	15.2
Dec-2006	9	48	-42	-7.4	17.2
Jan-2007	7	34	0	-3.3	26.4
Feb-2007	10	76	-16	-4.7	21.6
Mar-2007	12	105	-20	-4.7	17.6
Apr-2007	15	109	-38	-6.4	13.2
May-2007	21	141	-31	-5.2	10.6
Jun-2007	24	184	-63	-8.7	6.6
Jul-2007	27	675	-67	-9	5
Aug-2007	29	176	-43	-5.7	2.6
Sep-2007	27	81	-30	-4.9	9.2
Oct-2007	21	135	n.d.	n.d.	n.d.
Nov-2007	13	31	-27	-6.9	28.2
Dec-2007	9	67	-25	-5.6	19.8
Jan-2008	7	137	n.d.	n.d.	n.d.
Feb-2008	5	44	n.d.	n.d.	n.d.
Mar-2008	11	91	n.d.	n.d.	n.d.
Apr-2008	16	116	-42	-6.7	11.8
May-2008	20	210	-54	-7.1	2.8
Jun-2008	23	776	-66	-9.1	6.7
Jul-2008	29	204	-67	-9.2	7.2
Aug-2008	28	227	-53	-7.9	10.7
Sep-2008	26	295	-79	-11.2	10.4
Oct-2008	20	62	-9	-5.1	32.4
Nov-2008	13	89	-11	-8.2	54.9
Dec-2008	8	106	-11	-3.6	17.8
Jan-2009	6	55	-21	-5.4	21.8
Feb-2009	10	134	-15	-4.3	18.8
Mar-2009	11	145	-32	-5.4	11.9
Apr-2009	16	80	-42	-6.8	13.2
May-2009	21	69	-37	-5.3	5.6
Jun-2009	24	246	-45	-6.7	8.9
Jul-2009	27	429	-53	-7.8	10.1
Aug-2009	29	67	-53	-7.1	4.2
Sep-2009	26	34	-27	-4.7	10.6
Oct-2009	19	130	-35	-5.0	5.2
Nov-2009	13	112	-69	-10.2	12.1
Dec-2009	8	67	-44	-7.9	19.4
Jan-2010	6	48	-25	-5.3	17.2
Feb-2010	10	192	-25	-4.6	12.0
Mar-2010	11	177	-25	-6.7	29.1
Apr-2010	15	226	-27	-4.5	8.5
May-2010	20	285	-29	-4.6	8.2
Jun-2010	24	401	-85	-11.6	7.9
Jul-2010	27	362	-42	-6.0	5.9
Aug-2010	30	58	-43	-5.5	1.3
Sep-2010	26	118	-43	-6.5	9.2
Oct-2010	20	85	-40	-6.7	13.3
Nov-2010	12	29	-34	-7.2	22.9
Dec-2010	8	94	-40	-7.7	21.1

month	average temperature (℃)	precipitation total amount(mm)	δD (‰)	$\delta^{18}O$ (‰)	d-excess (‰)
Jan-2011	3	3	-40	-8.6	28.2
Feb-2011	8	40	-58	-10.0	21.9
Mar-2011	8	51	-30	-6.7	23.7
Apr-2011	15	67	-14	-4.1	18.6
May-2011	20	126	-79	-10.3	4.2
Jun-2011	24	929	-69	-10.0	10.8
Jul-2011	28	253	-50	-7.4	9.4
Aug-2011	28	385	-44	-6.6	9.0
Sep-2011	25	76	-74	-9.8	4.8
Oct-2011	19	107	-40	-6.8	14.0
Nov-2011	16	89	-38	-6.9	16.6
Dec-2011	7	33	n.d.	n.d.	n.d.
Jan-2012	5	15	-64	-10.1	16.6
Feb-2012	6	32	-33	-6.3	17.5
Mar-2012	11	90	-21	-4.2	12.0
Apr-2012	16	42	-38	-5.8	9.1
May-2012	21	25	-61	-7.9	2.1
Jun-2012	23	223	-53	-7.4	6.8
Jul-2012	28	183	-41	-6.5	11.0
Aug-2012	29	35	-55	-8.1	9.7
Sep-2012	25	24	-74	-10.0	5.9
Oct-2012	19	39	-22	-5.1	18.0
Nov-2012	12	21	-35	-7.0	21.3
Dec-2012	6	14	-16	-4.9	24.0
Jan-2013	5	45	-96	-13.3	10.9
Feb-2013	7	167	-23	-5.5	20.7
Mar-2013	12	110	-17	-4.0	15.8
Apr-2013	15	164	-19	-4.4	15.8
May-2013	21	54	-30	-4.8	8.2
Jun-2013	24	308	-57	-8.5	10.6
Jul-2013	29	119	-38	-6.2	11.8
Aug-2013	29	571	-52	-7.8	11.0
Sep-2013	25	199	-89	-12.7	12.7
Oct-2013	21	109	-43	-6.6	9.1
Nov-2013	12	80	-35	-6.7	18.8
Dec-2013	7	51	-68	-10.1	13.1
Jan-2014	6	36	-18	-5.4	25.5
Feb-2014	7	121	-41	-7.5	19.0
Mar-2014	11	130	-35	-6.1	13.2
Apr-2014	16	69	-14	-3.5	14.5
May-2014	20	135	-50	-7.4	9.1
Jun-2014	23	259	-84	-11.3	6.6
Jul-2014	27	358	-31	-4.4	4.6
Aug-2014	27	213	-48	-7.4	11.0
Sep-2014	24	107	-52	-7.9	11.5
Oct-2014	20	142	-29	-5.3	13.8
Nov-2014	14	63	-40	-7.1	16.7
Dec-2014	6	63	-23	-6.6	29.4
Jan-2015	7	100	-31	-6.1	17.6
Feb-2015	7	34	-21	-5.3	21.0
Mar-2015	11	186	-23	-5.7	22.2
Apr-2015	17	151	-11	-2.9	11.8
May-2015	21	131	-36	-5.7	9.7
Jun-2015	22	628	-39	-6.4	11.8
Jul-2015	26	376	-53	-8.0	10.8
Aug-2015	27	246	-61	-8.6	8.1
Sep-2015	24	150	-64	-9.2	9.5
Oct-2015	19	65	-70	-10.0	10.2
Nov-2015	16	137	2	-2.7	22.9
Dec-2015	10	92	-49	-8.2	16.2
Jan-2016	6	71	-20	-5.0	19.7
Feb-2016	7	74	-64	-10.3	18.3
Mar-2016	11	60	-35	-7.2	22.8
Apr-2016	17	179	-47	-8.3	19.7
May-2016	21	273	-37	-7.1	20.6
Jun-2016	24	644	-5	-2.5	15.1
Jul-2016	28	390	-19	-3.8	11.6

ARTICLE IN PRESS

Geologia Croatica

ARTICLE IN PRESS